Ninety million years of orogenesis, 250 million years of quiescence and further orogenesis with no change in PT: Significance for the role of deformation in porphyroblast growth

A A Shah[1,2,*] and T H Bell[1]

[1]*School of Earth and Environmental Sciences, James Cook University, Townsville, Qld 4811, Australia.*
[2]*Earth Observatory of Singapore, Nanyang Technological University, Singapore.*
Corresponding author. e-mail: afroz@ntu.edu.sg

In situ dating of monazite grains preserved as inclusions within foliations defining FIAs (foliation inflection/intersection axes preserved within porphyroblasts) contained within garnet, staurolite, andalusite and cordierite porphyroblasts provides a chronology of ages that matches the FIA succession for the Big Thompson region of the northern Colorado Rocky Mountains. FIA sets 1, 2 and 3 trending NE–SW, E–W and SE–NW were formed at 1760.5 ± 9.7, 1719.7 ± 6.4 and 1674 ± 11 Ma, respectively. For three samples where garnet first grew during just one of each of these FIAs, the intersection of Ca, Mg, and Fe isopleths in their cores indicate that these rocks never got above 4 kbars throughout the Colorado Orogeny. Furthermore, they remained around approximately the same depth for ∼250 million years to the onset of the younger Berthoud Orogeny at 1415 ± 16 Ma when the pressure decreased slightly as porphyroblasts formed with inclusion trails preserving FIA set 4 trending NNE–SSW. No porphyroblast growth occurred during the intervening ∼250 million years of quiescence, even though the PT did not change over this period. This confirms microstructural evidence gathered over the past 25 years that crenulation deformation at the scale of a porphyroblast is required for reactions to re-initiate and enable further growth.

1. Introduction

In multiply deformed and metamorphosed rocks, foliations in the matrix, especially schistosity parallel to compositional layering, have generally undergone long and complex histories (e.g., Ham and Bell 2004). Different relics of this history can be left in strain shadows or portions where later deformation partitioning was less pervasive and if not decoded carefully will lead to erroneous or ambiguous results (e.g., Spiess and Bell 1996). Each new deformation tends to erase developing or earlier-formed structures through decrenulation of developing crenulation cleavage and rotation of relics of earlier-formed foliations into parallelism with the compositional layering (e.g., Bell *et al.* 2003). Deformation partitioning strongly affects such kinds of processes from regional (Cihan and Parsons 2005) to porphyroblastic scales (Bell and Bruce 2007) and makes it difficult to correlate them from one region to another. It is primarily because a mixture of ages will always be present within matrix of such rocks and gets even worst if deformation partitioning was intense. The inclusion trails preserved within porphyroblasts are remnants of earlier matrix events. These are

Keywords. FIAs; porphyroblast; monazite; garnet; staurolite.

generally isolated from the matrix phases and act as robust candidates for studying deformation and metamorphic processes. Such quantitative research has greatly increased our understanding of complex inclusion trail relationships, which otherwise could not be interpreted or were misleading (e.g., Ham and Bell 2004).

Accurate measurement of the foliation inflection/intersection axes preserved within different porphyroblastic phases (FIAs) has made it possible to decode lengthy and complex histories of deformation and metamorphism in orogens around the world (e.g., Bell *et al.* 2004). More than 10 years of research and data have already been published using this technique from tectonically complex regions around the world (e.g., Bell *et al.* 1998, 2003, 2005; Bell and Chen 2002; Cihan 2004; Kim and Bell 2005; Sayab 2005, 2006; Bell and Bruce 2007; Sanislav 2010; Sanislav and Shah 2010; Ali 2010; Sanislav and Bell 2011).

The integration of detailed microstructural studies and FIA data with garnet isopleth thermobarometry/MnNCKFMASH pseudosection construction can provide complete pressure–temperature–time deformational trajectories of an area (e.g., Kim and Bell 2005; Cihan *et al.* 2006; Sayab 2006; Ali 2010). Such an approach significantly improves our understanding of large-scale orogenic processes. But the absolute timing of these events remains a fundamental tool for decoding and interpreting the tectonic evolution of the region. Geometrically and texturally controlled dating methods are critical for constraining the ages of deformed and metamorphosed sediments and their textures and foliations (e.g., Williams and Jercinovic 2002). In pelites and psammites, monazite is commonly present at amphibolite facies (Dahl *et al.* 2005) and it has been dated in migmatites and granulites (e.g., Kelly *et al.* 2006). It is considered as a typical mineral of choice for *in situ* geochronology in such rocks (Dahl *et al.* 2005; Williams *et al.* 2007).

Absolute dating of monazite grains applying high precission electron microprobe U-Th-Pb techniques (EPMA) was used to correlate different metamorphic and deformational events (e.g., Montel *et al.* 1996; Dahl *et al.* 2005) because the bulk of the monazite grains analysed were smaller in size. Dating of monazite inclusions within different FIA sets (Bell and Welch 2002; Ali 2010; Sanislav 2010; Sanislav and Shah 2010) provides a robust tool for understanding and unravelling lengthy and complex orogenic histories. Integration of FIAs with this approach provides a strong basis for studying the complex pressure–temperature–time-deformation (PT–t-D) paths that rocks appear to have followed. This paper reports the results obtained from adapting this approach to the rocks collected in and around the Big Thompson region of Colorado (figures 1 and 2).

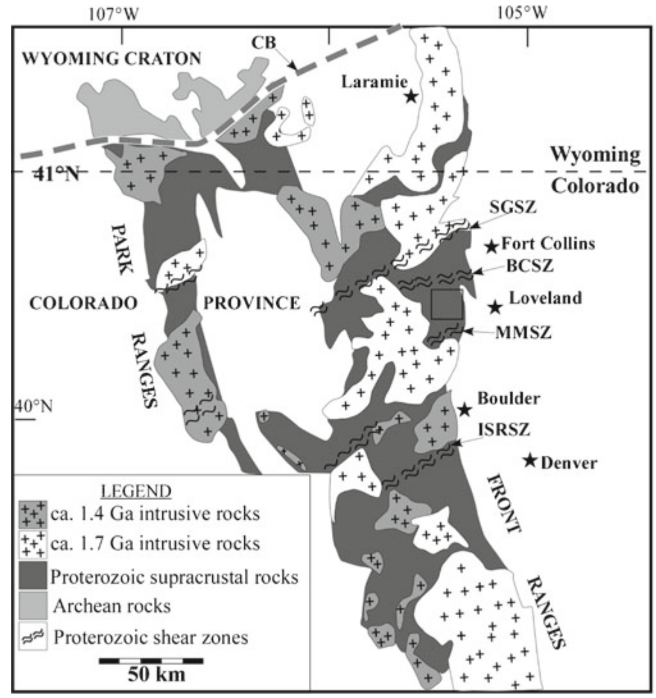

Figure 1. Regional map of the Colorado Frontal Range showing the Precambrian rocks and the location of the study area (box shows area of figure 2). BCSZ: Buckhorn Creek shear zone, CB: Cheyenne belt, ISRSZ: Idaho Springs-Ralston shear zone, MMSZ: Moose Mountain shear zone, SGSZ: Skin Gulch shear zone (modified after Cavosie and Selverstone 2003).

2. Regional geology and tectonics

The rocks exposed in the Big Thomson Canyon region, Colorado, USA, are mainly metasediments and granitoids (figure 2). Condie and Martel (1983) suggested that the metasediments represent mature sediments deposited in a forearc setting. Reed *et al.* (1987) argued that they were possibly deposited in a back-arc setting between two ∼1.8 and 1.7 Ma magmatic arc systems. Recent detrital zircon ages suggest a maximum age of 1758+26 Ma for deposition of the Big Thompson sequence (Selverstone *et al.* 2000). These sediments were repeatedly deformed, metamorphosed and intruded by various plutons (e.g., Braddock and Cole 1979; Selverstone *et al.* 1997; Sims *et al.* 2003) during the Colorado (∼1700 Ma) and Berthoud (∼1400 Ma) orogenies (Tweto 1987; Nyman *et al.* 1994; Karlstrom *et al.* 1997). The rocks show an increase in metamorphic grade towards the west and north and three stages of folding and cleavage development (Cavosie and Selverstone 2003).

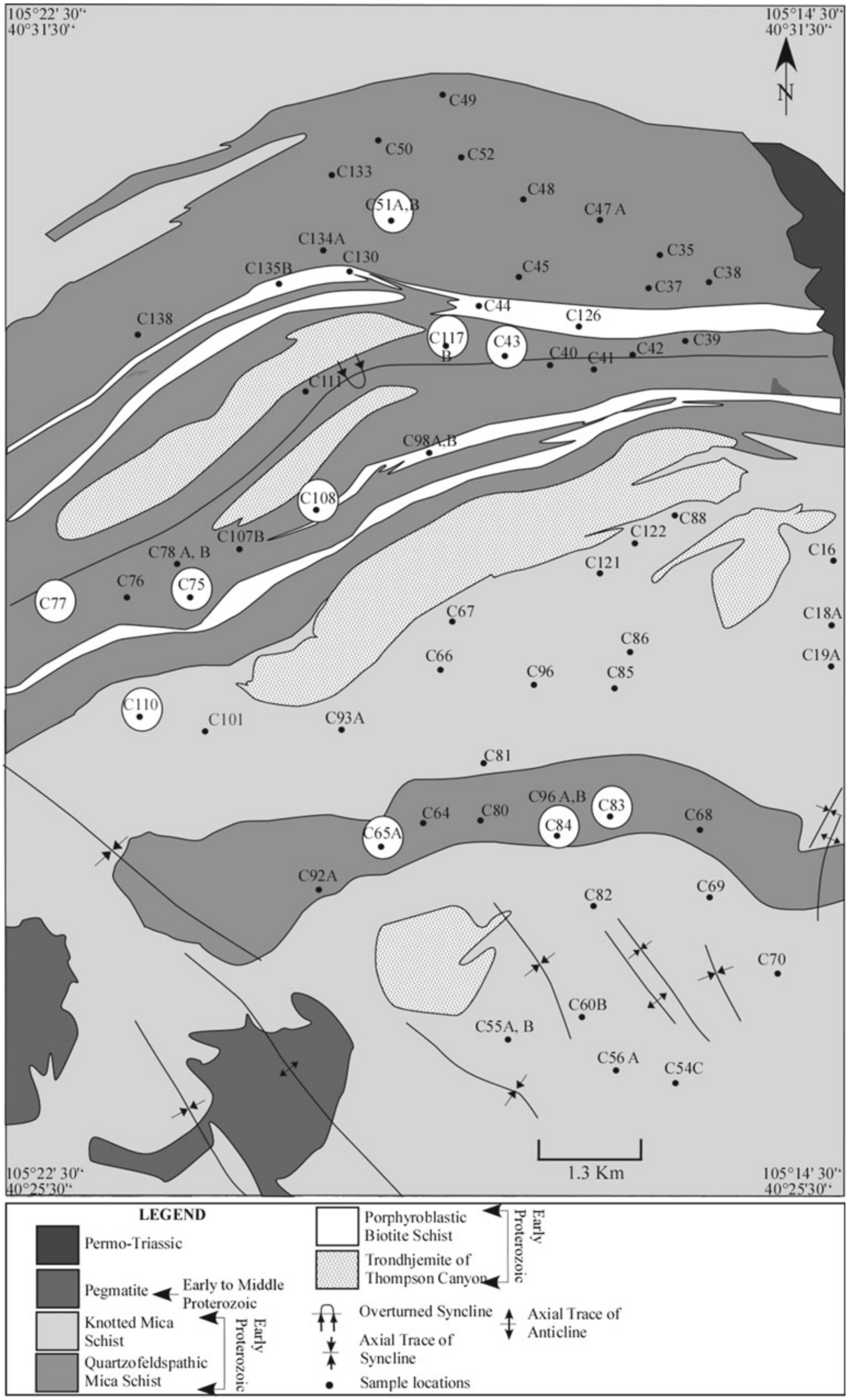

Figure 2. Detailed geological map of the study area and the sample locations. White circles show the location of samples used for monazite dating (geological map modified after Cavosie and Selverstone 2003).

The first deformation/metamorphism occurred before 1750 Ma and resulted in large-scale isoclinal folds (F1) and a regional axial cleavage S1. The second and third stages of folding (F2 and F3) occurred around 1750 Ma ago, when these rocks were intruded by the Boulder Creek granodiorite and related rocks. Only one period of metamorphism has been associated with these events (M1) during which garnet and staurolite grew. The second metamorphic event (M2), which was stronger than the first, resulted in the formation of up to sillimanite grade mineral assemblages (Sims *et al.* 2003), though metamorphic conditions were very heterogeneous throughout these episodes. A number of areas recorded an entire transition in metamorphic grade from the chlorite zone to the onset of migmatization during the Colorado orogeny (Braddock and Cole 1979; Selverstone *et al.* 1997).

3. Methods

3.1 *FIA measurements*

Hayward (1990) and Bell *et al.* (1995, 1998) described a technique for analysing the geometries of inclusion trails within porphyroblasts. It involves measurement of the FIA, which is achieved by cutting a minimum of eight vertically oriented thin sections around the compass from each rock sample to locate the switch in inclusion trail asymmetry (clockwise or anticlockwise) within the porphyroblasts (figure 3a and b). Where the FIA trends vary from the core to the rim of the porphyroblasts, a relative timing and thus an FIA succession can be established (Bell *et al.* 1998). The accumulated error associated with determining the trend of the FIA in each rock is random, and is estimated to be ±8 in both situations when one uses a COCLAR compass (see Bell *et al.* 1998).

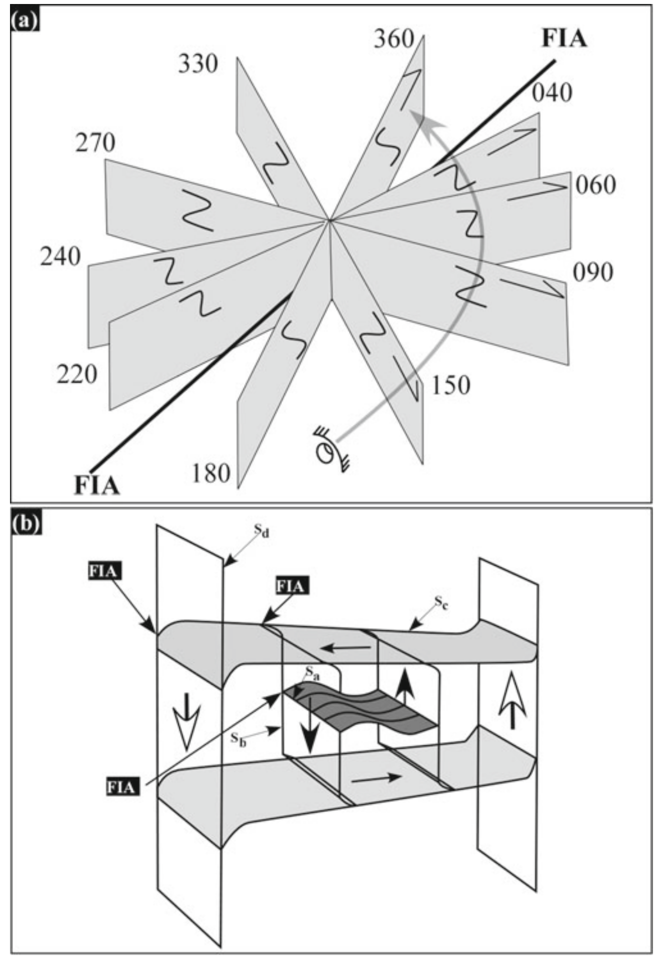

Figure 3. (**a**) Sketch illustrating the method developed by Bell *et al.* (1995, 1998) by which the trend of an FIA is measured. This technique uses the change in asymmetries of inclusion trails in a porphyroblast, when viewed in a consistent direction for successive striking vertical thin sections, to locate the FIA. The inclusion trail asymmetry changes between 0° and 40°. Thin section orientation is marked as single barbed arrow. The eyeball and grey arrow indicates the direction in which the sections are viewed. (**b**) The 3-D sketch illustrates a succession of foliations, as they would be preserved within a vertical slice through a porphyroblast, which define a single FIA trend.

4. Results

4.1 *FIA data*

A total of 67 oriented samples were examined for the present research. 800 oriented thin sections were prepared and a total of 138 FIA and pseudo-FIA trends were determined (table 1, figure 2). These measurements were achieved by cutting a minimum of eight vertically oriented thin sections around the compass from each rock sample (figure 3) and then locating the switch in inclusion trail asymmetry (clockwise or anticlockwise) within the porphyroblasts (e.g., Bell *et al.* 1998).

Garnet, staurolite, andalusite and cordierite porphyroblasts preserve earlier foliations as inclusion trails. These foliations are most commonly straight with curvature at their extremities (e.g., figure 4a). Porphyroblast inclusion trails are commonly truncated (e.g., figure 4a) by the matrix foliations but some are not (e.g., figure 4b). A relative timing and thus an FIA succession can be established from samples preserving an FIA trend that varies from core to the rim of the porphyroblast (e.g., Bell *et al.* 1998). All FIA measurements are plotted on rose diagram and are shown in figure 5(a). A total of 64 and 53 FIAs were measured in garnet and staurolite porphyroblasts respectively (figure 5b and c).

Table 1. *Samples collected in and around Big Thompson Canyon region of northern Front Range, Colorado (shown in figure 2), the geological formations from which they were taken, their latitude and longitude values and the FIA trends measured in them.*

Sample	Easting	Northing	FM	Garnet single FIA	pFIA	Core	Rim	Staurolite single FIA	pFIA	Cordierite single FIA	pFIA	Andalusite single FIA
C16	N			15								
C18A	N			15								
C18B	N			15	130							
C19A	N			15	135							
C35	477206	4484713	XKS	55				25				
C37	477144	4484332	XBS	140				30				
C38	477712	4484329	XKS					15				
C39	477339	4483694	XKS	90				20				
C40	475828	4483433	XKS	85	50			135				
C41	476404	4483291	XKS					30				
C42	476752	4483561	XKS	55				25				
C43	475001	4483553	XKS	50				80				
C44	474752	4484140	XKS	80				15	130			
C45	475338	4484548	XKS	85				140				
C47A	476418	4485315	XKS	140				25				
C48	475216	4485600	XKS					135				
C49	474307	4486810	XKS					90		120		
C50	473290	4486411	XKS					135		25		25
C51A	473670	4485437	XKS	130								
C51B	473670	4485437	XKS	55						125		
C52	474484	4485910	XQS			50	85			25		
C54C	476858	4474303	XQS	25				25				
C55A	474470	4475194	XQS	55								
C55B	474470	4475194	XQS	40				15				
C56A	475827	4474568	XQS	45				125				
C60B	475036	4475308	XQS					85				
C64	473360	4477763	XKS	85	40			125				
C65A	472961	4477978	XQS	55				130	80			
C66	473717	4479430	XQS	50				120	40			
C67	473793	4480256	XQS			85	130					
C68A	476612	4477904	XKS					120				
C68B	476612	4477904	XKS	90	50							
C69	477142	4476720	XQS			130	25					
C70	477433	4475714	XQS	85								
C75	470687	4480815	XBS					85	60			
C76	469767	4480350	XQS			85	135			25		125
C77	469104	4480353	XQS								120	
C78A	470822	4479966	XQS	45				25		115		
C78B	470822	4479966	XQS	85	50			130		130		
C80	474017	4478095	XKS					85				
C81	474505	4478748	XQS	145				15				
C82	475584	4476971	XQS	125				30				
C83	475634	4477975	XKS	80				135				
C84	474792	4477824	XKS	85				130				
C85	475463	4479506	XQS	90				30				
C86	476096	4479964	XQS	125	50							
C88	476418	4481613	XQS	55				25				
C92A	472011	4477468	XKS	130								
C93A	472642	4479207	XQS	55				30				
C96A	475043	4479775	XQS	85				130				
C96B	475043	4479775	XQS			55	135					

Table 1. *(Continued)*

Sample	Easting	Northing	FM	Garnet single FIA	pFIA	Core	Rim	Staurolite single FIA	pFIA	Cordierite single FIA	pFIA	Andalusite single FIA
C98A	473791	4482058	XBS					55		25		
C98A	473791	4482058	XBS	55				90		30		
C101	470677	4478975	XKS	15	85					30		
C107B	471172	4481971	XKS	50				30		30		
C108	470558	4478720	XKS	50				85		20		
C110	471694	4482963	XKS	25					120			20
C111	472000	4483403	XKS					25	55			
C117B	474053	4483669	XKS	55				80		35		
C121	475042	4482626	XQS	85								
C122	475531	4482644	XBS					130				
C126	475980	4483996	XKS	55				120				
C130	472840	4484427	XKS					50				25
C133	472811	4485927	XKS					85	55			
C134A	472679	4485070	XKS	60				90				
C135B	472295	4484694	XKS	55				80				130
C138B	469858	4485392	XKS					65				135

XQS = Quartzofeldspathic mica schist, XKS = Knotted mica schist, XBS = Porphyroblastic biotite schist, N = No information available about the geographic coordinates.

The combined FIA trend data for garnet and staurolite is shown in figure 5(d). The other porphyroblastic phases in which FIAs were measured were andalusite and cordierite, with seven measurements in the former and 14 in the latter. Their trends are given in table 1 and are shown on a rose diagram in figure 5(e and f). A few samples maintain differentiated crenulation cleavages that have been overgrown by the porphyroblasts where the asymmetry of the crenulated cleavage can be determined. The crenulated cleavages consist of quartz and ilmenite grains, while the differentiated crenulation cleavages predominantly contain ilmenite grains. The intersection between the crenulated and crenulation cleavages can be determined, when viewed in three dimensions, and is called a pseudo-FIA (pseudo-FIA). The actual FIA is formed during porphyroblast growth and these samples are defined by the curvature of the differentiated crenulation cleavage. All measured trends were plotted on a rose diagram as shown in figure 5.

4.2 *Dating of FIA sets*

To determine the age of the four FIA sets measured in the area, 30 samples were selected for monazite dating. Polished thin sections were made for use in the JEOL JXA-8300 Superprobe. Only 11 samples out of the 30 selected contained monazite grains large enough for precise age calculations. Detailed pre-dating maps were produced from each polished thin section to accurately locate monazite grain and their textural setting. The analytical procedure is outlined in table 2. The samples were analysed with a 1–2 micron meter diameter beam at 15 kv and 200 nA. The collimators were opened to a maximum (3 mm) and the PHA settings were optimized as well. In all these measurements, πrz matrix corrections were performed using standard Pb, U, Th, and Y concentrations in combination with the preset values for other elements (P 33.3, La 14.5, Ce 26, Pr 2.6, Nd 10.3, Sm 1.5, Gd 1.48, Dy 0.82, Si 0.25, Ca 0.55 wt.% oxides). Interference corrections of Th and Y on Pb Mα and Th on U Mβ were executed as in Pyle *et al.* (2002). An internal standard monazite from Manangotry in Madagascar of 545 ± 2 Ma (Paquette *et al.* 1984) was analysed three times before and after each analytical session. Chemical ages were calculated as described in Montel *et al.* (1996). Geologically significant age information can be derived by assuming low amounts of common Pb (e.g., Parrish 1990; Gaidies *et al.* 2008) and slow diffusion rates for Th, U and Pb in monazite (Cherniak *et al.* 2004). The samples were chosen based on FIA set and the grains were isolated and clustered according to their age, textural setting and whether any chemical zonation was present (Cihan *et al.* 2006). This would potentially reduce any error and make the age information reliable (Montel *et al.* 1996; Pyle *et al.* 2005; Gaidies *et al.* 2008). Dates and errors were determined by mean age with standard errors at 95% confidence level for a cluster of spots analysis within a single age domain or grain. Ages were

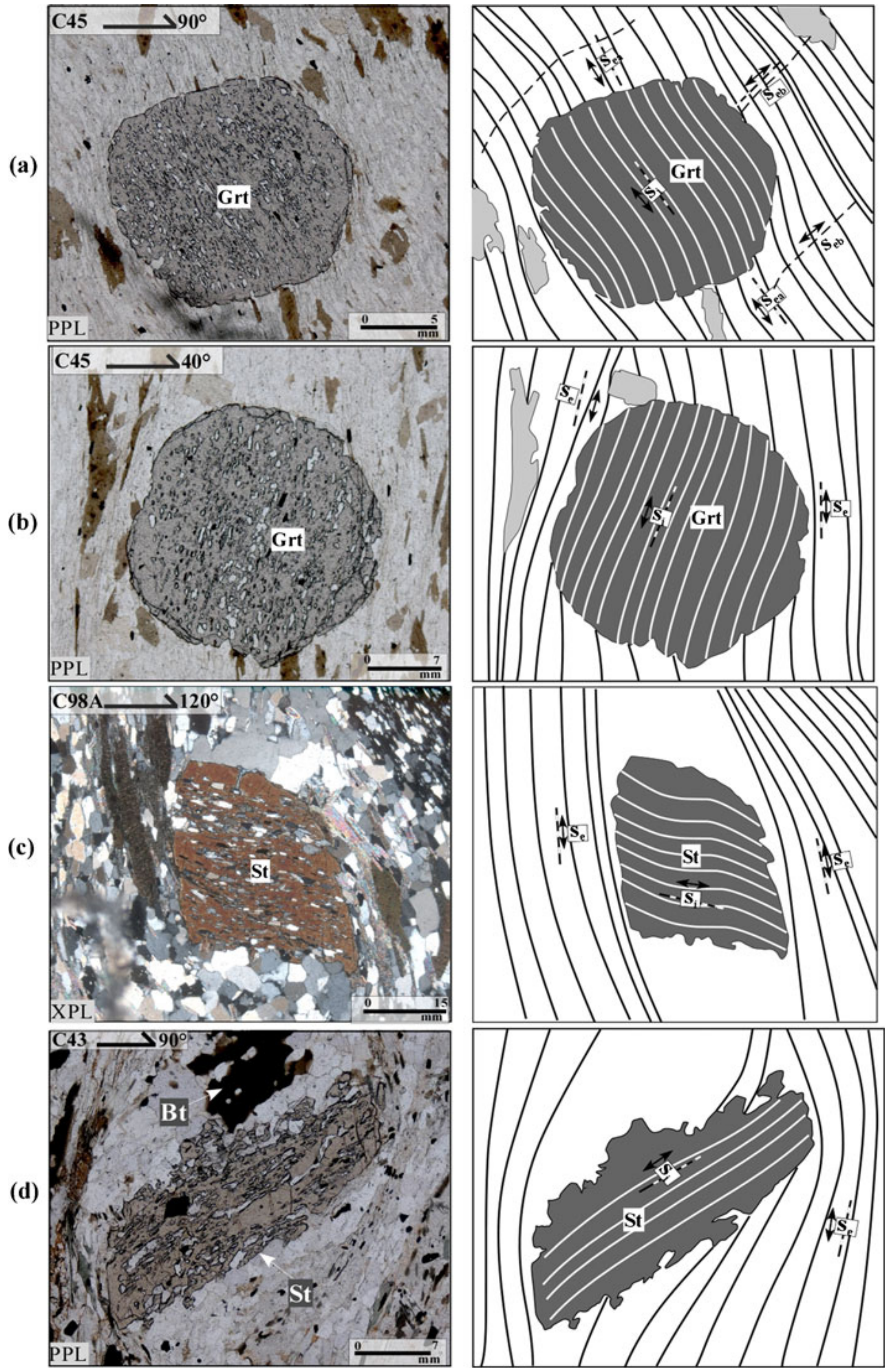

Figure 4. Representative photomicrographs and line diagrams of vertical thin sections of different samples illustrating variation in inclusion trail geometry, truncation and continuity with the matrix foliation. (**a**, **b**) Garnet porphyroblast preserves an oblique foliation that curves clockwise to sub-vertical (S_i). (**c**, **d**) Garnet porphyroblast preserves a sub-horizontal foliation (S_i) truncated and curved by a sub-vertical with an anti-clockwise asymmetry. (**e**, **f**) Staurolite porphyroblast preserves a sub-horizontal foliation (S_i) that is truncated with that in the matrix and has an anti-clockwise curvature. (**g**, **h**) Staurolite porphyroblast with inclusion trails completely truncated by those within the matrix. A slightly anti-clockwise curvature was observed in the rim or from the porphyroblast into the matrix in these porphyroblasts. Sample numbers, strikes and way up of the vertical thin sections are shown in the upper left corner (thick single barbed arrow). PPL: plane polarized light; XPL: cross polarized light, S_e: external foliation, S_i: Internal foliation, St: staurolite, Bt: biotite, Grt: garnet (after Shah 2009).

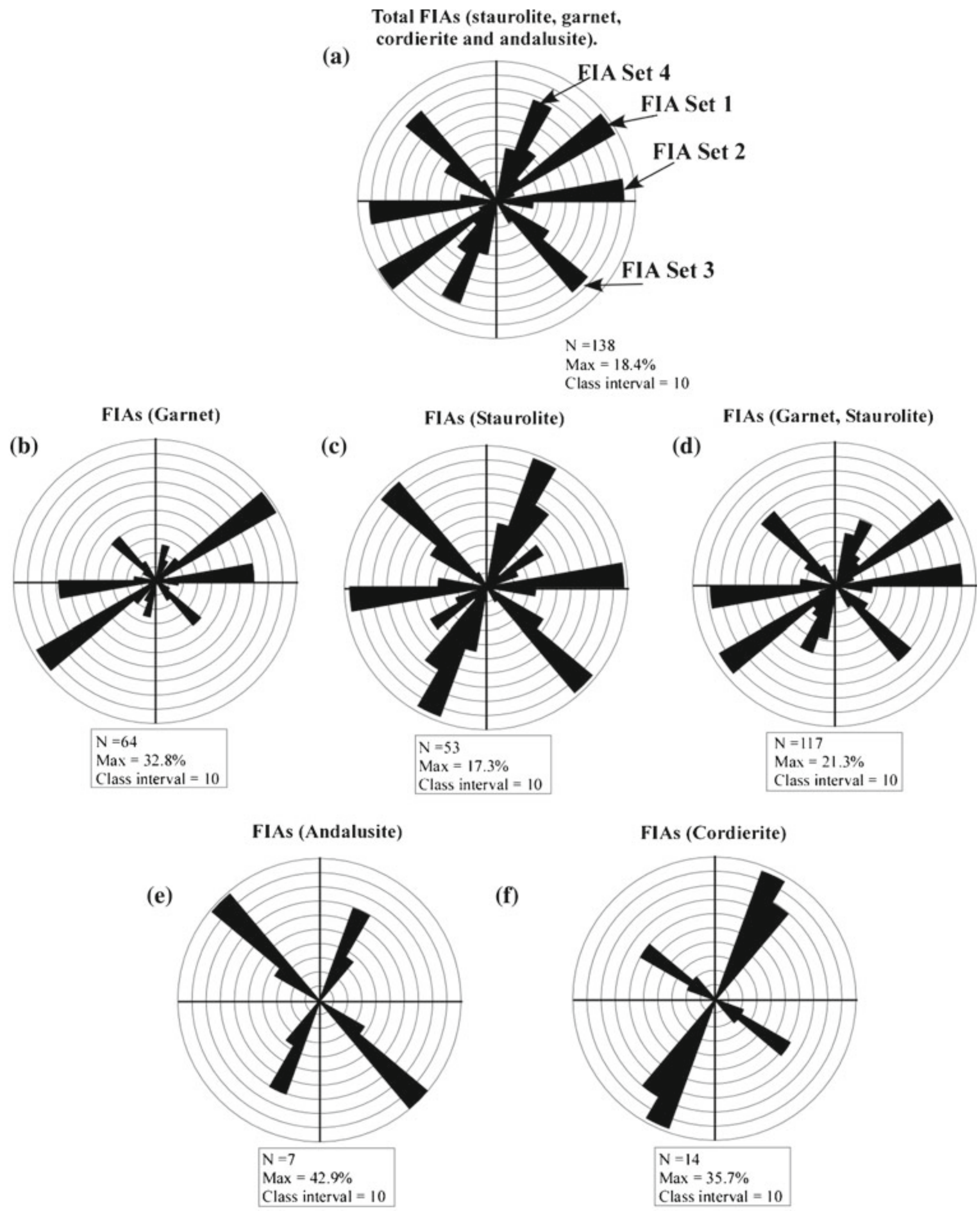

Figure 5. (**a**) Equal area rose plot of all FIA trends measured from garnet, staurolite, andalusite and cordierite. Four peaks occur at 25°, 55°, 85° and 135°. (**b**) Garnet FIAs (**c**) staurolite FIAs, (**d**) garnet plus staurolite FIAs, (**e**) andalusite FIAs, and (**f**) cordierite FIAs.

then calculated for all the grain populations analyzed and plotted using software Isoplot (Ludwig 1998). Three samples contained monazite grains big enough to extract valuable age information in garnet porphyroblasts. Six contained suitable monazite grains in staurolite porphyroblasts. Two contained suitable monazite grains in andalusite plus cordierite.

4.3 *Dating of foliations within porphyroblasts*

Unless otherwise stated, monazite inclusions lie with the foliation defining the FIA set for that mineral phase. All rocks contain biotite, muscovite, plagioclase and quartz with accessory phases ilmenite and apatite. Quartz and apatite and rarely muscovite, biotite, chlorite inclusions are always present within both garnet and staurolite porphyroblasts. Monazite is always present within staurolite but not necessarily in garnet phases.

4.3.1 *Sample C117*

Garnet (FIA set 1) and staurolite (FIA set 2) inclusion trails are always truncated by the matrix

Table 2. *Analytical set-up for monazite analyses on the JEOL JXA-8200, Electron Probe Micro Analyzer (EPMA) at the Advanced Analytical Centre, JCU Townsville, Australia.*

Element	X-ray	Crystal-spectrometer	Peak time (s)	Background time (s)	Standard
P	Ka	TAP	20	10	Ce phosphate
Pb	Ma	PETJ[b]	180	90	PbSiO3a[a]
La	La	LIFH	10	5	La phospahte
U	Mb	PETJ	180	90	Uranium[a]
Th	Ma	PETJ	90	45	ThO2[c]
Y	La	TAP	60	30	Yttrium phosphate[d]
Ce	La	LIFH	10	5	Ce phosphate
Ca	Ka	PETJ	20	10	Wollastonite
Si	Ka	TAP	20	10	PbSiO3
Pr	Lb	LIFH	20	10	Pr phosphate
S	Ka	PETJ	30	15	BaSO4
Nd	Lb	LIFH	10	5	Nd phosphate
Sm	Lb	LIFH	40	20	Sm phospahte
Gd	Lb	LIFH	40	20	Gd phospahte
Dy	Lb	LIFH	40	20	DY phospate

[a]Astimex, [b]Sealed Xe detectors, [c]Taylor, [d]Pb-free synthetic from J. Pyle (Rennselaer Polytechnic Institute, USA).

Table 3. *Summary of ages derived from monazites preserved within the porphyroblasts and the matrix phases of above-mentioned samples (staurolite data from Sanislav and Shah 2010).*

	Porphyroblast					Matrix				
	Sample	Textural setting	Age and error	Total no. of spots	No. of monazites	Sample	Textural setting	Age and error	Total no. of spots	No. of monazites
FIA 1	C117B	Grt M1	1756 ± 22	17	2	C75	Bt M1	1664 ± 38	7	1
	C75	St M2	1765 ± 23	16	1	C75	Bt M2	1762 ± 35	7	1
	C84	Grt M3	1762 ± 21	24	1	C43	Mu M3	1724 ± 37	7	1
	C77	Crd M4	1760 ± 18	24	1	C108	Mt[a] M4	1675 ± 24	10	1
	C51B	Crd M5	1762 ± 32	12	1	C77	Bt M5	1677 ± 19	17	1
						C51B	Mt M6	1685 ± 29	9	1
FIA 2	C43	St M6	1724 ± 19	14	1	C84	Mt[a] M7	1729 ± 23	26	1
	C65A	St M7, 8, 9	1717.6 ± 9.5	53	3	C83	Mu M8	1723 ± 34	7	1
	C108	St M10, 11	1721 ± 14	37	2	C110	Mu M9	1438 ± 30	7	1
	C77	Crd M12	1726 ± 18	22	1	C65	Bt M10	1665 ± 23	10	1
	C75	St M13	1712 ± 25	10	1	C65	Bt M11	1742 ± 29	8	1
						C65	Mt[a] M11	1668 ± 48	6	1
FIA 3	C83	St M14	1681 ± 27	10	1					
	C51A	Grt M15	1666 ± 26	10	1	[a]Mt = Matrix				
	C77	And M16	1678 ± 17	20	1					
	C84	St M17	1683 ± 36	6	1					
	C65	St M18	1665 ± 24	10	1					
FIA 4	C51 B	Crd M19	1414 ± 23	13	1					
	C77	Crd M20	1410 ± 26	10	1					
	C110	And M21	1432 ± 39	5	1					

foliation. Extra minor phases include zircon and xenotine. Two monazite inclusions within garnet have given a mean age spread of 1756 ± 22 Ma (see tables 3 and 4; figure 6).

4.3.2 *Sample C84*

Garnet and staurolite inclusion trails are always truncated by the matrix foliation. Extra accessory

Table 4. *Complete data about the chemical analyses of all monazite grains, preserved within porphyroblasts and matrix phases of samples aligned to FIA set 1.*

Shah S.No.	P_2O_5	PbO	La_2O_3	UO_2	ThO_2	Y_2O_3	Ce_2O_3	CaO	SiO_2	Pr_2O_3	SO_3	Nd_2O_3	Sm_2O_3	Gd_2O_3	Dy_2O_3	Total	Sample[a]	Age	Error
Monazite within porphyroblast																			
Shah S.No. 1	31.451	0.515	13.431	0.627	4.320	1.340	28.098	1.055	0.185	3.176	0.000	11.971	1.971	1.990	0.507	100.637	C117B Grt M1 1	**1772**	**69**
Shah S.No. 2	31.225	0.428	13.853	0.365	4.280	1.076	28.745	0.935	0.234	3.157	0.008	11.971	1.951	1.833	0.475	100.537	C117B Grt M1 2	**1736**	**78**
Shah S.No. 3	31.451	0.421	14.127	0.421	3.920	0.988	28.559	0.909	0.201	3.147	0.020	12.294	2.078	2.029	0.381	100.948	C117B Grt M1 3	**1755**	**80**
Shah S.No. 4	31.422	0.395	14.196	0.453	3.460	1.136	28.980	0.821	0.147	3.265	0.008	12.137	2.029	1.912	0.417	100.778	C117B Grt M1 4	**1757**	**84**
Shah S.No. 5	31.637	0.298	14.471	0.319	2.600	1.038	29.608	0.625	0.143	3.284	0.008	12.618	2.108	2.000	0.360	101.116	C117B Grt M1 5	**1796**	**110**
Shah S.No. 6	31.588	0.280	14.314	0.361	2.370	1.087	29.980	0.620	0.128	3.314	0.017	12.382	2.000	1.863	0.444	100.747	C117B Grt M1 6	**1728**	**108**
Shah S.No. 7	31.657	0.269	14.255	0.331	2.260	1.151	29.990	0.591	0.105	3.392	0.006	12.608	2.000	1.863	0.441	100.918	C117B Grt M1 7	**1762**	**116**
Shah S.No. 8	31.333	0.515	13.147	0.320	5.650	0.988	27.706	1.124	0.338	3.069	0.016	11.882	2.088	2.255	0.515	100.945	C117B Grt M1 8	**1722**	**67**
Shah S.No. 9	31.902	0.442	13.598	0.366	4.330	1.380	28.255	0.946	0.227	3.069	0.012	11.882	2.000	2.216	0.744	101.368	C117B Grt M1 9	**1773**	**78**
Shah S.No. 10	31.618	0.390	13.549	0.463	3.380	1.158	28.667	0.791	0.179	3.186	0.012	12.216	2.029	2.069	0.621	100.328	C117B Grt M1 10	**1748**	**83**
Shah S.No. 11	31.529	0.338	13.569	0.288	3.380	1.280	29.039	0.744	0.192	3.206	0.000	12.275	2.147	2.294	0.693	100.974	C117B Grt M1 11	**1738**	**94**
Shah S.No. 12	31.461	0.312	13.745	0.310	2.920	1.340	29.127	0.670	0.137	3.275	0.008	12.480	2.088	2.235	0.709	100.818	C117B Grt M1 12	**1753**	**102**
Shah S.No. 13	31.314	0.337	13.794	0.431	2.880	1.059	29.127	0.692	0.169	3.265	0.011	12.225	1.980	1.922	0.647	99.852	C117B Grt M1 13	**1723**	**92**
Shah S.No. 14	31.422	0.315	13.961	0.360	2.800	1.197	29.206	0.657	0.145	3.324	0.005	12.363	2.010	2.069	0.629	100.461	C117B Grt M1 14	**1744**	**99**
Shah S.No. 15	31.814	0.302	14.049	0.293	2.750	1.269	29.422	0.622	0.172	3.294	0.012	12.265	2.069	2.127	0.643	101.101	C117B Grt M1 15	**1795**	**107**
Shah S.No. 16	31.873	0.266	14.118	0.243	2.390	1.122	29.931	0.564	0.115	3.363	0.010	12.314	2.059	2.059	0.655	101.080	C117B Grt M1 16	**1839**	**124**
Shah S.No. 17	32.088	0.249	14.245	0.296	2.090	0.948	30.255	0.508	0.114	3.392	0.027	12.569	1.990	1.912	0.552	101.235	C117B Grt M1 17	**1786**	**125**
Shah S.No. 34	31.402	0.442	13.618	0.386	4.310	1.360	28.245	0.886	0.272	3.216	0.000	12.196	1.902	1.539	0.539	100.313	C84 Grt M3 1	**1759**	**77**
Shah S.No. 35	31.412	0.434	13.686	0.404	4.200	1.360	28.373	0.878	0.292	3.245	0.006	12.265	1.902	1.559	0.642	100.657	C84 Grt M3 2	**1742**	**77**
Shah S.No. 36	31.324	0.396	13.578	0.457	3.520	1.650	28.118	0.808	0.243	3.265	0.012	12.206	2.039	1.735	0.675	100.024	C84 Grt M3 3	**1738**	**82**
Shah S.No. 37	31.363	0.398	13.696	0.513	3.430	1.600	28.647	0.828	0.189	3.235	0.000	12.265	1.971	1.686	0.621	100.442	C84 Grt M3 4	**1711**	**79**
Shah S.No. 38	31.206	0.352	14.206	0.361	3.240	1.360	28.882	0.692	0.180	3.265	0.013	11.990	2.000	1.598	0.481	99.827	C84 Grt M3 5	**1758**	**92**
Shah S.No. 39	31.578	0.377	14.029	0.468	3.020	1.610	28.637	0.741	0.226	3.304	0.001	12.265	2.039	1.696	0.696	100.688	C84 Grt M3 6	**1809**	**88**
Shah S.No. 40	31.225	0.339	13.951	0.435	2.740	1.570	28.735	0.645	0.139	3.314	0.005	12.333	2.039	1.696	0.602	99.771	C84 Grt M3 7	**1780**	**95**
Shah S.No. 41	31.382	0.305	13.951	0.335	2.720	1.520	29.225	0.655	0.205	3.412	0.002	12.578	2.020	1.706	0.624	100.641	C84 Grt M3 8	**1758**	**102**
Shah S.No. 42	31.637	0.288	14.343	0.309	2.560	1.320	29.304	0.596	0.207	3.275	0.006	12.265	1.931	1.549	0.511	100.101	C84 Grt M3 9	**1777**	**109**
Shah S.No. 43	31.451	0.281	14.167	0.284	2.560	1.290	29.696	0.601	0.177	3.382	0.007	12.539	1.990	1.539	0.565	100.529	C84 Grt M3 10	**1773**	**111**
Shah S.No. 44	31.235	0.268	14.304	0.289	2.310	1.320	29.569	0.523	0.111	3.314	0.015	12.284	2.010	1.559	0.499	99.608	C84 Grt M3 11	**1804**	**118**
Shah S.No. 45	31.549	0.251	14.775	0.311	2.100	1.300	30.098	0.519	0.115	3.324	0.012	12.500	1.971	1.559	0.588	100.970	C84 Grt M3 12	**1764**	**121**
Shah S.No. 46	30.951	0.258	14.676	0.331	2.090	1.340	29.627	0.487	0.162	3.392	0.004	12.422	1.971	1.578	0.543	99.832	C84 Grt M3 13	**1776**	**118**
Shah S.No. 47	31.559	0.239	14.520	0.297	2.020	1.340	29.951	0.491	0.092	3.392	0.005	12.441	1.990	1.529	0.587	100.452	C84 Grt M3 14	**1749**	**124**
Shah S.No. 48	31.441	0.237	14.392	0.284	2.010	1.340	29.647	0.499	0.127	3.392	0.022	12.647	2.020	1.608	0.552	100.218	C84 Grt M3 15	**1765**	**127**
Shah S.No. 49	31.255	0.241	14.441	0.311	1.960	1.310	29.951	0.486	0.110	3.402	0.019	12.716	2.029	1.578	0.582	100.391	C84 Grt M3 16	**1772**	**125**
Shah S.No. 50	31.402	0.231	14.647	0.309	1.880	1.340	30.029	0.484	0.108	3.431	0.000	12.608	1.990	1.559	0.636	100.655	C84 Grt M3 17	**1749**	**128**

Shah S.No. 51	30.833	0.417	13.520	0.566	3.240	1.620	27.598	0.933	0.254	3.196	0.002	11.931	2.010	1.647	0.679	98.447	C84 Grt M3 18	**1784**	**80**
Shah S.No. 52	31.029	0.301	14.186	0.382	2.560	1.390	28.873	0.679	0.169	3.304	0.006	12.422	2.000	1.588	0.621	99.509	C84 Grt M3 19	**1734**	**101**
Shah S.No. 53	31.186	0.288	14.343	0.377	2.520	1.360	29.275	0.645	0.177	3.343	0.013	12.402	2.000	1.588	0.604	100.122	C84 Grt M3 20	**1688**	**101**
Shah S.No. 54	30.373	0.283	13.765	0.330	2.470	1.340	28.686	0.602	0.551	3.216	0.007	12.245	1.990	1.471	0.522	97.849	C84 Grt M3 21	**1752**	**108**
Shah S.No. 55	31.637	0.272	13.863	0.312	2.380	1.430	29.147	0.585	0.347	3.363	0.013	12.451	2.069	1.598	0.607	100.073	C84 Grt M3 22	**1758**	**113**
Shah S.No. 56	31.549	0.264	14.343	0.297	2.200	1.300	29.627	0.526	0.255	3.353	0.013	12.559	2.020	1.559	0.578	100.443	C84 Grt M3 23	**1820**	**121**
Shah S.No. 57	31.216	0.246	14.010	0.223	2.140	1.250	29.039	0.529	0.614	3.255	0.003	12.284	1.961	1.500	0.565	98.834	C84 Grt M3 24	**1885**	**135**
Shah S.No. 58	30.210	0.485	13.970	0.396	5.020	1.320	28.170	1.061	0.313	3.100	0.005	11.660	1.970	1.860	0.569	100.108	C77 Crd M4 1	**1710**	**71**
Shah S.No. 59	30.440	0.512	13.650	0.545	4.560	1.700	27.960	1.076	0.187	3.120	0.013	11.430	1.990	1.870	0.745	99.797	C77 Crd M4 2	**1777**	**71**
Shah S.No. 60	30.620	0.482	13.590	0.527	4.230	1.680	27.690	1.020	0.208	3.080	0.004	11.610	2.020	1.810	0.767	99.339	C77 Crd M4 3	**1779**	**73**
Shah S.No. 61	30.530	0.450	13.840	0.490	4.160	1.580	28.090	0.970	0.159	3.010	0.014	11.690	2.030	1.880	0.642	99.536	C77 Crd M4 4	**1724**	**75**
Shah S.No. 62	30.640	0.456	13.580	0.515	4.150	1.680	28.020	1.004	0.182	3.170	0.007	11.690	2.070	1.850	0.729	99.743	C77 Crd M4 5	**1723**	**74**
Shah S.No. 63	30.560	0.442	13.510	0.474	3.960	1.680	28.160	0.928	0.175	3.150	0.002	11.820	2.060	1.870	0.718	99.508	C77 Crd M4 6	**1764**	**79**
Shah S.No. 64	30.640	0.425	13.620	0.432	3.960	1.580	28.130	0.963	0.175	3.090	0.010	11.590	2.020	1.840	0.709	99.183	C77 Crd M4 7	**1746**	**80**
Shah S.No. 65	30.260	0.431	13.740	0.488	3.870	1.540	28.250	0.969	0.170	3.250	0.004	11.620	1.910	1.730	0.680	98.911	C77 Crd M4 8	**1737**	**78**
Shah S.No. 66	30.620	0.463	14.030	0.508	3.830	1.630	28.350	0.931	0.178	3.170	0.001	11.810	2.010	1.890	0.691	100.111	C77 Crd M4 9	**1844**	**80**
Shah S.No. 67	30.430	0.442	13.970	0.479	3.820	1.660	28.390	0.918	0.163	3.090	0.008	11.610	1.980	1.850	0.695	99.505	C77 Crd M4 10	**1802**	**80**
Shah S.No. 68	30.090	0.388	13.980	0.429	3.340	1.570	28.790	0.806	0.146	3.100	0.000	11.740	1.980	1.800	0.712	98.871	C77 Crd M4 11	**1794**	**89**
Shah S.No. 69	30.430	0.355	14.190	0.377	3.320	1.540	29.140	0.779	0.160	3.160	0.000	11.990	2.020	1.830	0.707	99.999	C77 Crd M4 12	**1724**	**91**
Shah S.No. 70	30.230	0.372	14.010	0.408	3.300	1.540	28.720	0.805	0.130	3.190	0.000	11.910	1.950	1.830	0.760	99.156	C77 Crd M4 13	**1766**	**90**
Shah S.No. 71	30.550	0.392	13.890	0.431	3.220	1.630	28.500	0.786	0.146	3.170	0.017	11.890	2.030	1.840	0.699	99.192	C77 Crd M4 14	**1850**	**91**
Shah S.No. 72	30.520	0.340	14.030	0.337	3.160	1.460	28.980	0.747	0.341	3.240	0.000	11.950	2.040	1.750	0.680	99.576	C77 Crd M4 15	**1763**	**97**
Shah S.No. 73	30.500	0.298	14.370	0.323	2.750	1.460	29.380	0.649	0.112	3.260	0.000	12.360	2.030	1.870	0.624	99.985	C77 Crd M4 16	**1727**	**105**
Shah S.No. 74	30.520	0.282	14.720	0.320	2.660	1.370	29.890	0.640	0.098	3.260	0.014	11.920	2.000	1.770	0.610	100.074	C77 Crd M4 17	**1685**	**107**
Shah S.No. 75	30.610	0.278	14.810	0.322	2.540	1.380	29.760	0.623	0.104	3.230	0.007	12.010	2.040	1.850	0.664	100.228	C77 Crd M4 18	**1708**	**109**
Shah S.No. 76	30.610	0.297	14.950	0.330	2.520	1.430	29.610	0.651	0.112	3.260	0.000	12.080	2.040	1.900	0.569	100.358	C77 Crd M4 19	**1809**	**112**
Shah S.No. 77	30.450	0.281	14.360	0.302	2.520	1.430	29.680	0.613	0.099	3.210	0.013	12.000	1.960	1.760	0.661	99.338	C77 Crd M4 20	**1763**	**114**
Shah S.No. 78	30.470	0.274	14.670	0.276	2.500	1.350	29.680	0.595	0.114	3.200	0.006	12.150	1.970	1.770	0.545	99.568	C77 Crd M4 21	**1774**	**117**
Shah S.No. 79	30.610	0.264	14.880	0.295	2.330	1.330	29.910	0.585	0.095	3.180	0.007	11.950	2.000	1.810	0.600	99.846	C77 Crd M4 22	**1762**	**119**
Shah S.No. 80	30.390	0.221	15.220	0.251	2.090	1.246	30.260	0.509	0.083	3.240	0.003	11.770	1.950	1.640	0.549	99.422	C77 Crd M4 23	**1682**	**131**
Shah S.No. 81	30.490	0.233	14.790	0.263	2.010	1.310	30.120	0.519	0.071	3.260	0.010	12.190	1.940	1.690	0.704	99.601	C77 Crd M4 24	**1780**	**135**
Shah S.No. 82	31.200	0.266	14.900	0.359	2.050	1.243	29.160	0.520	0.148	3.290	0.015	12.650	2.040	1.600	0.547	99.988	C51B Crd M5 1	**1793**	**121**
Shah S.No. 83	30.700	0.347	15.020	0.872	1.200	2.020	29.110	0.523	0.109	3.240	0.007	12.340	1.920	1.630	0.698	99.735	C51B Crd M5 2	**1791**	**89**
Shah S.No. 84	30.500	0.314	15.890	0.895	0.925	1.650	29.710	0.415	0.084	3.270	0.005	12.210	1.920	1.510	0.616	99.913	C51B Crd M5 3	**1707**	**91**
Shah S.No. 85	30.590	0.254	15.400	0.810	0.428	2.300	29.500	0.523	0.069	3.310	0.004	12.440	1.860	1.550	0.692	99.729	C51B Crd M5 4	**1713**	**106**

Table 4. *(Continued)*

Shah S.No.	P_2O_5	PbO	La_2O_3	UO_2	ThO_2	Y_2O_3	Ce_2O_3	CaO	SiO_2	Pr_2O_3	SO_3	Nd_2O_3	Sm_2O_3	Gd_2O_3	Dy_2O_3	Total	Sample[a]	Age	Error
Shah S.No. 86	30.550	0.199	15.780	0.613	0.415	2.180	29.570	0.345	0.170	3.270	0.000	12.360	1.940	1.580	0.663	99.635	C51B Crd M5 5	**1707**	**131**
Shah S.No. 87	30.780	0.202	15.960	0.620	0.389	2.140	29.610	0.360	0.070	3.300	0.000	12.400	1.710	1.550	0.677	99.768	C51B Crd M5 6	**1733**	**131**
Shah S.No. 88	30.840	0.223	15.400	0.673	0.375	1.820	29.920	0.333	0.104	3.380	0.000	12.790	1.980	1.590	0.562	99.990	C51B Crd M5 7	**1782**	**125**
Shah S.No. 89	30.840	0.263	15.300	0.806	0.359	2.470	29.350	0.425	0.154	3.230	0.000	12.320	1.870	1.520	0.761	99.668	C51B Crd M5 8	**1796**	**109**
Shah S.No. 90	30.700	0.250	15.150	0.761	0.333	2.460	29.130	0.362	0.216	3.280	0.000	12.800	1.890	1.630	0.762	99.723	C51B Crd M5 9	**1809**	**114**
Shah S.No. 91	30.670	0.134	16.320	0.413	0.264	1.300	30.680	0.206	0.065	3.370	0.006	12.610	1.950	1.410	0.547	99.943	C51B Crd M5 10	**1717**	**191**
Shah S.No. 92	31.220	0.295	15.100	0.987	0.208	2.320	29.390	0.395	0.151	3.290	0.003	12.580	1.930	1.590	0.705	100.163	C51B Crd M5 11	**1752**	**95**
Shah S.No. 93	30.360	0.306	15.320	1.003	0.162	2.280	29.090	0.558	0.164	3.290	0.002	12.510	1.930	1.510	0.756	99.241	C51B Crd M5 12	**1801**	**94**
Monazite within matrix																			
Shah S.No. 94	30.931	0.529	13.451	0.410	5.140	1.290	27.382	1.088	0.296	3.078	0.007	12.010	1.863	1.559	0.533	99.568	C75 M 2 2	**1810**	**69**
Shah S.No. 95	31.245	0.485	13.716	0.434	4.590	1.450	27.255	1.005	0.280	3.137	0.013	11.990	2.029	1.716	0.549	99.895	C75 M 2 3	**1785**	**73**
Shah S.No. 96	31.382	0.238	14.441	0.277	2.110	1.290	29.686	0.525	0.100	3.333	0.002	12.431	1.971	1.637	0.594	100.018	C75 M 2 4	**1739**	**125**
Shah S.No. 97	31.294	0.229	14.373	0.276	2.090	1.300	29.882	0.500	0.073	3.402	0.020	12.706	2.108	1.676	0.554	100.482	C75 M 2 5	**1686**	**124**
Shah S.No. 98	31.422	0.227	14.363	0.262	2.110	1.245	29.902	0.479	0.083	3.373	0.001	12.676	2.059	1.588	0.592	100.381	C75 M 2 6	**1691**	**126**
Shah S.No. 99	31.147	0.203	14.382	0.250	1.820	1.280	30.010	0.445	0.077	3.392	0.002	12.637	2.049	1.618	0.600	99.911	C75 M 2 7	**1695**	**138**
Shah S.No. 101	31.314	0.486	12.922	0.359	4.950	0.632	27.598	1.065	0.236	3.157	0.012	12.167	2.275	2.294	0.542	100.009	65A M11 1	**1767**	**72**
Shah S.No. 102	31.520	0.386	13.480	0.285	3.900	0.690	28.255	0.849	0.194	3.147	0.000	12.333	2.235	2.284	0.594	100.153	65A M11 2	**1778**	**88**
Shah S.No. 103	31.382	0.390	13.167	0.374	3.850	1.510	28.324	0.865	0.246	3.078	0.022	12.000	2.078	2.235	0.817	100.340	65A M11 3	**1707**	**81**
Shah S.No. 104	31.490	0.375	13.294	0.322	3.830	0.705	28.412	0.853	0.181	3.176	0.008	12.186	2.255	2.392	0.628	100.108	65A M11 4	**1709**	**85**
Shah S.No. 105	31.412	0.393	13.529	0.334	3.760	0.882	28.225	0.851	0.173	3.137	0.011	11.990	2.118	2.402	0.789	100.006	65A M11 5	**1793**	**87**
Shah S.No. 106	31.314	0.458	13.431	0.709	3.490	0.620	29.118	0.955	0.106	3.186	0.007	12.333	2.196	1.755	0.272	99.950	65A M11 6	**1719**	**71**
Shah S.No. 107	31.216	0.379	14.078	0.479	3.190	0.359	30.010	0.825	0.115	3.343	0.008	12.569	2.147	1.529	0.232	100.480	65A M11 7	**1748**	**85**
Shah S.No. 108	31.422	0.295	13.804	0.284	2.900	1.280	29.245	0.681	0.112	3.216	0.015	12.343	2.049	2.059	0.709	100.413	65A M11 8	**1711**	**103**

[a] Sample number, porphyroblast and monazite.

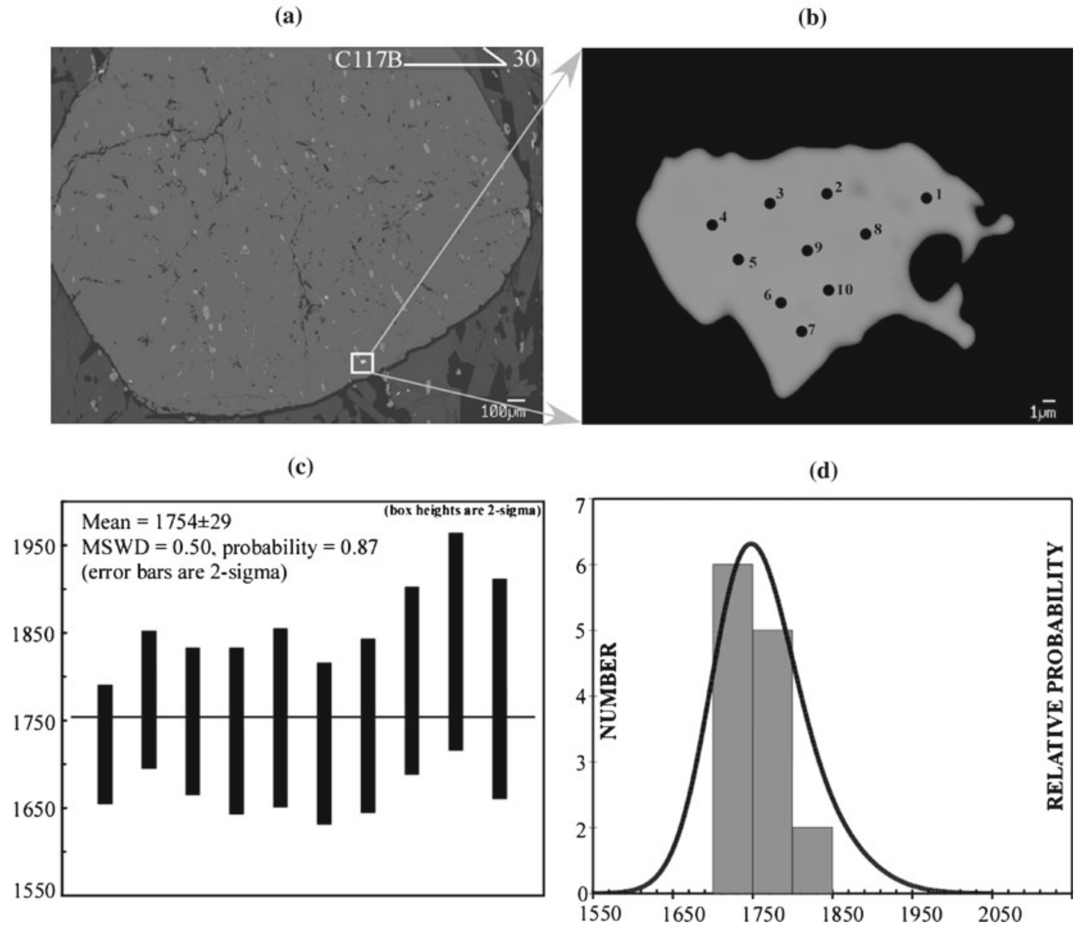

Figure 6. (**a**) Back scatter image shows the garnet porphyroblast which preserves a single monazite grain lying parallel to the orientation of its foliation. A mean age of 1754 ± 29 Ma is calculated from a total of 10 spots analyzed. (**b**) Enlarged view of the monazite grain with black spots showing the location of each analysis. In (**c**) the weighted average age plot is shown, created by using Isoplot software (Ludwig 1998) and in (**d**) the probability density plot is shown.

phases include magnetite, zircon, xenotine and monazite. A total of two monazite grains were dated from this sample. One within garnet with an age spread of 1762 ± 21 Ma (FIA set 1) and the other grain within staurolite (FIA set 3, Sanislav and Shah 2010) with an age spread of 1683 ± 36 Ma (see tables 3 and 4).

4.3.3 *Sample C77*

This sample contains andalusite and cordierite porphyroblasts, but no garnet and staurolite porphyroblasts, and the extra accessory phases of magnetite and xenotine. Inclusion trails in cordierite are continuous with the matrix foliation and preserve FIA set 4. Cordierite contains a pseudo-FIA belonging to set 3 and FIA set 4. Andalusite contains inclusion trails defining FIA set 3 that are truncated by foliations within both the matrix and the youngest foliation in cordierite. Inclusions in both porphyroblastic phases include staurolite and garnet although the latter is rare. Three monazite grains enclosed within cordierite (2) and andalusite (1) porphyroblasts were dated. One monazite grain within a crenulated cleavage seam gives a pseudo-FIA set 3 age of 1678 ± 17 Ma within cordierite. The andalusite porphyroblast preserves the same foliation as FIA 3. The 1760 ± 18 and 1726 ± 18 Ma ages were derived from their monazites (see tables 3–6).

4.3.4 *Sample C110*

Also contains andalusite and cordierite porphyroblasts. Extra accessory phases are dominated by magnetite, xenotine, zircon and baddeleyite. Andalusite preserves FIA set 4 and its inclusion trails are continuous with the matrix foliation. Inclusions within andalusite include staurolite and cordierite. A single monazite grain found in andalusite gave an age of 1432 ± 39 Ma (see tables 3 and 7) for the foliation preserved as inclusion trails.

Table 5. *Complete data about the chemical analyses of all monazite grains, preserved within porphyroblasts and matrix phases of samples aligned to FIA set 2.*

Shah S.No.	P_2O_5	PbO	La_2O_3	UO_2	ThO_2	Y_2O_3	Ce_2O_3	CaO	SiO_2	Pr_2O_3	SO_3	Nd_2O_3	Sm_2O_3	Gd_2O_3	Dy_2O_3	Total	Sample[a]	Age	Error
Monazite within Porphyroblast																			
Shah S.No.105	31.294	0.596	12.471	0.790	5.010	2.250	26.706	1.277	0.210	3.010	0.023	11.461	2.029	2.176	0.710	100.013	C77 crd M12 1	**1721**	**58**
Shah S.No.106	31.324	0.359	14.265	0.490	2.970	1.630	29.873	0.871	0.137	3.157	0.005	11.422	1.843	1.833	0.622	100.800	C77 crd M12 2	**1721**	**87**
Shah S.No.107	31.696	0.318	14.078	0.388	2.850	1.690	29.676	0.752	0.106	3.275	0.003	11.990	1.971	2.039	0.612	101.443	C77 crd M12 3	**1699**	**95**
Shah S.No.108	31.343	0.294	14.294	0.357	2.410	1.520	30.618	0.760	0.109	3.284	0.007	11.912	1.863	1.853	0.541	101.165	C77 crd M12 4	**1794**	**108**
Shah S.No.109	31.657	0.266	14.206	0.349	2.230	1.650	30.098	0.614	0.074	3.275	0.000	12.127	1.961	1.961	0.616	101.083	C77 crd M12 5	**1728**	**112**
Shah S.No.110	31.598	0.245	14.088	0.352	1.970	1.670	29.990	0.525	0.076	3.167	0.000	12.206	2.039	2.059	0.579	100.565	C77 crd M12 6	**1715**	**120**
Shah S.No.111	30.350	0.541	13.230	0.539	5.010	1.760	27.390	1.171	0.257	3.080	0.004	11.810	2.070	1.900	0.740	101.177	C77 crd M12 7	**1762**	**67**
Shah S.No.112	30.360	0.479	13.330	0.493	4.660	1.690	27.510	1.033	0.200	3.110	0.000	11.570	2.070	1.910	0.746	100.945	C77 crd M12 8	**1692**	**70**
Shah S.No.113	30.550	0.428	13.600	0.385	4.250	1.560	28.280	0.969	0.191	3.130	0.016	11.840	1.990	1.860	0.764	100.973	C77 crd M12 9	**1727**	**79**
Shah S.No.114	30.220	0.400	13.940	0.372	3.970	1.470	28.340	0.897	0.201	3.180	0.001	12.000	2.030	1.820	0.663	100.954	C77 crd M12 10	**1714**	**82**
Shah S.No.115	30.340	0.479	13.940	0.692	3.840	1.640	28.410	1.035	0.108	3.060	0.009	11.660	1.810	1.650	0.655	100.619	C77 crd M12 11	**1716**	**70**
Shah S.No.116	30.380	0.383	13.810	0.362	3.810	1.510	28.640	0.873	0.162	3.240	0.000	12.040	1.970	1.780	0.695	101.363	C77 crd M12 12	**1704**	**85**
Shah S.No.117	30.340	0.390	13.960	0.383	3.790	1.470	28.540	0.863	0.144	3.160	0.016	11.990	1.910	1.780	0.712	100.788	C77 crd M12 13	**1715**	**84**
Shah S.No.118	30.450	0.391	13.950	0.358	3.760	1.520	28.470	0.827	0.177	3.140	0.010	11.980	2.040	1.820	0.707	101.332	C77 crd M12 14	**1757**	**87**
Shah S.No.119	30.430	0.380	13.870	0.362	3.750	1.490	28.880	0.839	0.156	3.270	0.009	12.310	2.030	1.880	0.646	101.297	C77 crd M12 15	**1710**	**85**
Shah S.No.120	30.500	0.395	13.740	0.386	3.740	1.550	28.630	0.852	0.132	3.200	0.005	12.150	2.000	1.930	0.765	101.623	C77 crd M12 16	**1748**	**86**
Shah S.No.121	30.450	0.383	13.720	0.370	3.670	1.530	28.490	0.837	0.134	3.170	0.006	12.140	2.000	1.850	0.730	101.261	C77 crd M12 17	**1739**	**87**
Shah S.No.122	30.480	0.380	13.840	0.356	3.650	1.490	28.880	0.835	0.150	3.200	0.000	12.200	2.040	1.860	0.667	100.487	C77 crd M12 18	**1746**	**88**
Shah S.No.123	30.420	0.355	13.910	0.363	3.580	1.480	28.760	0.826	0.142	3.230	0.004	12.200	2.000	1.790	0.693	100.155	C77 crd M12 19	**1656**	**87**
Shah S.No.124	30.550	0.341	14.090	0.287	3.350	1.400	29.060	0.751	0.166	3.190	0.002	12.310	1.950	1.830	0.641	100.575	C77 crd M12 20	**1765**	**98**
Shah S.No.125	30.400	0.286	14.090	0.247	2.840	1.370	29.730	0.646	0.147	3.290	0.011	12.410	2.040	1.760	0.598	100.776	C77 crd M12 21	**1741**	**111**
Shah S.No.126	30.400	0.277	14.200	0.252	2.710	1.360	29.470	0.633	0.172	3.250	0.007	12.330	2.050	1.760	0.630	100.376	C77 crd M12 22	**1736**	**115**
Monazite within matrix																			
Shah S.No.137	31.588	0.270	13.990	0.326	2.420	1.760	28.980	0.603	0.120	3.373	0.008	12.412	2.108	2.000	0.679	100.637	C43 M3 1	**1709**	**108**
Shah S.No.138	31.794	0.313	13.931	0.380	2.760	1.830	28.569	0.648	0.133	3.255	0.005	12.392	2.088	1.980	0.676	100.755	C43 M3 2	**1721**	**97**
Shah S.No.139	32.020	0.250	14.353	0.302	2.300	1.620	29.500	0.568	0.130	3.343	0.022	12.412	1.990	1.873	0.609	101.290	C43 M3 3	**1679**	**114**
Shah S.No.140	31.833	0.346	14.049	0.490	2.680	1.750	28.667	0.649	0.141	3.216	0.012	12.167	2.029	1.980	0.382	100.391	C43 M3 4	**1759**	**88**
Shah S.No.141	31.794	0.262	14.098	0.355	2.180	1.580	29.480	0.541	0.115	3.324	0.021	12.265	1.922	1.833	0.703	100.473	C43 M3 5	**1720**	**112**
Shah S.No.142	31.373	0.355	13.725	0.415	3.190	1.800	28.186	0.755	0.178	3.186	0.004	12.088	2.020	2.000	0.605	99.881	C43 M3 6	**1721**	**87**
Shah S.No.143	32.294	0.321	14.118	0.440	2.610	1.810	28.941	0.672	0.167	3.294	0.013	11.990	1.931	1.843	0.599	101.044	C43 M3 7	**1735**	**95**
Shah S.No.144	31.480	0.430	13.637	0.450	3.980	1.710	28.667	1.302	0.242	3.186	0.010	11.784	2.029	2.049	0.651	101.609	C84 M7 1	**1742**	**76**
Shah S.No.145	31.539	0.230	13.951	0.249	2.220	1.330	29.892	0.533	0.073	3.304	0.000	12.284	2.069	1.951	0.540	100.164	C84 M7 2	**1678**	**122**
Shah S.No.146	31.490	0.294	13.873	0.297	2.700	1.370	29.373	0.646	0.117	3.343	0.011	12.255	2.059	1.931	0.572	100.331	C84 M7 3	**1765**	**106**
Shah S.No.147	31.529	0.320	13.892	0.318	3.080	1.370	29.431	0.699	0.121	3.324	0.002	12.069	2.000	1.931	0.668	100.755	C84 M7 4	**1722**	**95**

Shah S.No.148	31.500	0.394	13.412	0.404	3.940	1.460	28.627	0.871	0.150	3.235	0.001	11.941	2.029	1.882	0.611	100.460	C84 M7 5	**1665**	**78**
Shah S.No.149	31.520	0.237	13.775	0.233	2.180	1.310	29.863	0.537	0.101	3.382	0.000	12.461	2.049	1.873	0.650	100.171	C84 M7 6	**1779**	**129**
Shah S.No.150	31.588	0.452	13.245	0.496	4.250	1.590	28.186	0.950	0.170	3.137	0.008	11.667	1.971	1.961	0.643	100.314	C84 M7 7	**1703**	**71**
Shah S.No.151	31.784	0.278	14.039	0.260	2.610	1.350	29.127	0.629	0.123	3.304	0.019	11.990	2.049	1.941	0.431	99.935	C84 M7 8	**1777**	**113**
Shah S.No.152	31.667	0.312	13.922	0.292	2.850	1.340	29.598	0.630	0.112	3.333	0.015	11.735	1.980	1.765	0.590	100.140	C84 M7 9	**1805**	**103**
Shah S.No.153	31.775	0.539	13.000	0.668	4.660	1.860	27.294	1.122	0.194	3.108	0.003	11.373	2.020	2.137	0.732	100.483	C84 M7 10	**1731**	**63**
Shah S.No.154	31.941	0.370	14.020	0.392	3.480	1.540	28.961	0.802	0.163	3.216	0.007	12.294	1.951	1.853	0.741	101.731	C84 M7 11	**1719**	**84**
Shah S.No.155	31.794	0.337	13.765	0.342	2.980	1.520	29.333	0.701	0.118	3.304	0.000	12.520	2.098	2.020	0.624	101.457	C84 M7 12	**1809**	**96**
Shah S.No.156	31.706	0.363	13.559	0.383	3.470	1.560	28.961	0.800	0.137	3.206	0.000	12.441	2.157	2.108	0.675	101.526	C84 M7 13	**1703**	**85**
Shah S.No.157	31.647	0.492	12.882	0.514	4.680	1.710	27.853	1.067	0.188	3.216	0.005	12.294	2.108	2.098	0.687	101.440	C84 M7 14	**1711**	**67**
Shah S.No.158	30.54	0.220	15	0.326	1.86	1.030	29.88	0.485	0.098	3.38	0.023	12.65	2.05	1.58	0.52	99.641	C51B M8 1	**1656**	**120**
Shah S.No.159	30.53	0.216	14.69	0.200	2.16	1.212	29.82	0.489	0.105	3.42	0.006	12.85	2.08	1.68	0.53	99.986	C51B M8 2	**1704**	**135**
Shah S.No.160	30.46	0.294	14.42	0.241	3.1	1.256	29.04	0.667	0.125	3.24	0.006	12.45	2.04	1.66	0.55	99.551	C51B M8 3	**1690**	**104**
Shah S.No.161	30.59	0.544	13.86	0.936	3.63	1.51	27.94	1.112	0.049	3.19	0.008	12.28	2.05	1.61	0.56	99.871	C51B M8 4	**1756**	**64**
Shah S.No.162	30.44	0.583	13.5	1.077	3.64	1.45	27.67	1.181	0.056	3.18	0.015	12.17	1.99	1.56	0.59	99.099	C51B M8 5	**1751**	**60**
Shah S.No.163	30.04	0.263	14.38	0.314	2.45	1.37	29.29	0.598	0.078	3.35	0	12.75	2.1	1.67	0.64	99.296	C51B M8 6	**1675**	**111**
Shah S.No.164	30.23	0.187	15.13	0.207	1.85	1.058	30.1	0.428	0.144	3.37	0.002	12.69	1.74	1.5	0.53	99.171	C51B M8 7	**1647**	**149**

[a] Sample number, porphyroblast and monazite.

4.3.5 *Sample C55A*

This sample also contains cordierite plus minor xenotine. Garnet preserves inclusion trails defining FIA set 3 that are truncated by the foliation in cordierite and the matrix. Cordierite contains FIA set 4 trails that are continuous with those present within the matrix. Staurolite is also included in cordierite. A single monazite dated at 1666 ± 26 Ma from this sample is located within garnet (see tables 3 and 6). No monazite grains were found in cordierite.

4.3.6 *Sample C51B*

This sample also contains cordierite porphyroblasts with inclusion trails defining FIA set 4 that are continuous with foliations preserved within the matrix. Staurolite and andalusite are also present as inclusions. Two grains of monazite dated at an average age of 1412 ± 17 Ma lie within the foliation preserved within the cordierite (see tables 3 and 7). Another monazite was dated at 1762 ± 32 Ma, within the same foliation (see tables 3 and 6).

5. Dating of matrix foliations

The foliations within porphyroblasts are completely truncated by those within the matrix phases in all samples except C110. Consequently, monazite ages in the matrix cannot be used to date FIAs. They were dated to see what relics of the deformation history determined from the FIA succession were preserved in the matrix and whether there was any evidence for deformation occurring between the Colorado and Berthoud orogenies.

5.1 *Sample C83 (FIA 2 in garnet and 3 in staurolite)*

A single monazite grain parallel to the main matrix foliation (S_{e1}) of this sample has an age of 1723 ± 34 Ma (see tables 3 and 5). This sample preserves FIA set 2 within garnet and set 3 in staurolite porphyroblasts (figure 7).

5.2 *Sample C75 (FIA 1 and 2 in staurolite)*

Three foliations in the matrix (S_{ea}–S_{ec}) are shown in figure 8. A 1664 ± 38 Ma age was derived from a monazite grain lying sub-parallel to S_{e2} (figure 9). Another monazite grain that lay orthogonal to this

Table 6. *Complete data about the chemical analyses of all monazite grains, preserved within porphyroblasts and matrix phases of samples aligned to FIA set 3.*

Shah S.No.	P_2O_5	PbO	La_2O_3	UO_2	ThO_2	Y_2O_3	Ce_2O_3	CaO	SiO_2	Pr_2O_3	SO_3	Nd_2O_3	Sm_2O_3	Gd_2O_3	Dy_2O_3	Total	Sample[a]	Age	Error
Monazite within Porphyroblast																			
Shah S.No.1	31.078	0.649	12.706	0.843	5.670	1.780	27.186	1.392	0.230	3.039	0.003	11.422	1.922	2.010	0.559	100.490	C51 A Grt M15 1	**1693**	**54**
Shah S.No.2	31.157	0.558	13.176	0.757	5.010	1.630	27.873	1.240	0.210	3.137	0.001	11.725	1.931	2.029	0.580	101.016	C51 A Grt M15 2	**1645**	**59**
Shah S.No.3	30.657	0.454	13.392	0.438	4.600	1.510	28.618	0.992	0.239	3.137	0.000	11.716	1.863	1.922	0.598	100.135	C51 A Grt M15 3	**1673**	**72**
Shah S.No.4	30.755	0.365	13.696	0.377	3.480	1.470	29.353	0.834	0.159	3.225	0.004	12.108	1.971	1.961	0.603	100.360	C51 A Grt M15 4	**1713**	**87**
Shah S.No.5	30.588	0.330	14.137	0.392	3.110	1.450	30.127	0.852	0.150	3.245	0.025	12.157	1.882	1.990	0.491	100.928	C51 A Grt M15 5	**1661**	**90**
Shah S.No.6	30.020	0.293	14.343	0.345	2.900	1.450	30.186	0.738	0.130	3.343	0.005	12.000	1.961	1.873	0.481	100.069	C51 A Grt M15 6	**1617**	**96**
Shah S.No.7	30.725	0.266	14.098	0.330	2.500	1.430	30.186	0.623	0.129	3.343	0.006	12.137	1.863	1.902	0.557	100.095	C51 A Grt M15 7	**1645**	**107**
Shah S.No.8	30.892	0.235	14.314	0.392	1.940	1.660	30.853	0.524	0.072	3.353	0.006	12.549	1.971	1.971	0.616	101.348	C51 A Grt M15 8	**1601**	**113**
Shah S.No.9	30.804	0.219	14.539	0.287	1.900	1.390	30.657	0.516	0.084	3.353	0.006	11.882	1.814	1.755	0.564	99.771	C51 A Grt M15 9	**1698**	**131**
Shah S.No.10	30.804	0.226	13.961	0.337	1.870	1.620	30.069	0.523	0.088	3.412	0.006	12.363	1.961	1.941	0.639	99.819	C51 A Grt M15 10	**1670**	**124**
Shah S.No.11	30.070	0.385	14.180	0.385	3.820	1.390	28.820	0.806	0.192	3.210	0.007	11.950	1.890	1.690	0.724	99.518	C77 And M16 1	**1682**	**83**
Shah S.No.12	30.450	0.373	14.060	0.361	3.820	1.390	28.910	0.840	0.181	3.150	0.005	11.610	1.960	1.720	0.646	99.476	C77 And M16 2	**1659**	**84**
Shah S.No.13	30.350	0.405	13.680	0.452	3.770	1.550	28.600	0.857	0.157	3.080	0.004	11.660	2.020	1.770	0.682	99.037	C77 And M16 3	**1704**	**80**
Shah S.No.14	30.270	0.388	13.690	0.499	3.740	1.480	28.690	0.894	0.476	3.150	0.005	11.670	1.910	1.580	0.575	99.017	C77 And M16 4	**1600**	**76**
Shah S.No.15	30.070	0.360	13.980	0.384	3.450	1.440	29.100	0.781	0.160	3.200	0.009	11.910	1.910	1.730	0.614	99.098	C77 And M16 5	**1693**	**88**
Shah S.No.16	30.500	0.308	14.170	0.349	2.860	1.420	29.290	0.646	0.136	3.180	0.008	11.830	2.000	1.750	0.709	99.156	C77 And M16 6	**1698**	**101**
Shah S.No.17	30.530	0.279	14.230	0.301	2.680	1.390	29.620	0.627	0.134	3.240	0.000	12.320	1.980	1.780	0.616	99.727	C77 And M16 7	**1684**	**108**
Shah S.No.18	30.510	0.270	14.230	0.317	2.600	1.350	29.690	0.616	0.114	3.270	0.007	11.880	1.960	1.730	0.657	99.201	C77 And M16 8	**1649**	**108**
Shah S.No.19	30.110	0.451	13.440	0.537	4.270	1.670	28.220	1.066	0.150	3.110	0.012	11.580	2.000	1.690	0.658	98.963	C77 And M16 9	**1657**	**71**
Shah S.No.20	30.070	0.420	14.170	0.512	3.940	1.530	28.640	0.979	0.133	3.090	0.012	11.380	1.870	1.550	0.596	98.891	C77 And M16 10	**1653**	**75**
Shah S.No.21	30.360	0.453	13.170	0.529	4.290	1.770	28.020	1.021	0.144	3.180	0.006	11.850	2.070	1.880	0.742	99.485	C77 And M16 11	**1666**	**71**
Shah S.No.22	30.250	0.420	13.670	0.448	4.020	1.620	28.390	0.921	0.167	3.180	0.000	11.840	1.990	1.800	0.656	99.372	C77 And M16 12	**1694**	**78**
Shah S.No.23	30.280	0.568	13.070	0.607	5.380	1.850	27.020	1.239	0.209	3.020	0.019	11.540	2.010	1.870	0.811	99.492	C77 And M16 13	**1707**	**62**
Shah S.No.24	30.220	0.465	13.570	0.423	4.670	1.520	28.340	0.999	0.243	3.160	0.016	11.540	1.970	1.640	0.656	99.432	C77 And M16 14	**1705**	**72**
Shah S.No.25	30.330	0.424	13.850	0.352	4.430	1.440	28.670	0.930	0.210	3.120	0.011	11.710	1.890	1.690	0.617	99.674	C77 And M16 15	**1695**	**78**
Shah S.No.26	30.310	0.383	14.030	0.399	3.770	1.490	28.600	0.853	0.166	3.130	0.000	11.790	2.020	1.800	0.684	99.425	C77 And M16 16	**1674**	**83**
Shah S.No.27	30.190	0.485	13.460	0.533	4.580	1.670	27.950	1.053	0.182	3.130	0.005	11.540	1.990	1.800	0.721	99.289	C77 And M16 17	**1698**	**69**
Shah S.No.28	30.530	0.492	13.600	0.551	4.670	1.690	28.330	1.094	0.207	3.130	0.000	11.940	1.980	1.780	0.753	100.746	C77 And M16 18	**1681**	**68**
Shah S.No.29	29.560	0.456	13.390	0.475	4.420	1.590	28.120	1.038	0.259	3.160	0.000	12.050	2.000	1.880	0.735	99.133	C77 And M16 19	**1691**	**73**
Shah S.No.30	30.230	0.401	13.660	0.420	3.990	1.580	28.480	0.910	0.525	3.130	0.000	11.800	1.950	1.820	0.713	99.609	C77 And M16 20	**1660**	**79**
Shah S.No.31	30.765	0.604	12.382	0.424	6.930	1.193	26.598	1.588	0.393	2.941	0.021	11.333	2.069	2.265	0.641	100.149	65A M18 1	**1631**	**56**
Shah S.No.32	31.245	0.501	13.147	0.276	5.670	1.053	27.608	1.195	0.362	3.049	0.015	11.667	2.049	2.098	0.562	100.497	65A M18 2	**1712**	**68**
Shah S.No.33	30.618	0.422	13.363	0.424	4.350	0.955	28.559	0.976	0.218	3.196	0.008	12.020	2.059	1.951	0.542	99.660	65A M18 3	**1638**	**73**
Shah S.No.34	31.216	0.417	13.343	0.450	3.980	0.934	29.020	0.871	0.218	3.118	0.013	12.059	2.078	1.961	0.544	100.220	65A M18 4	**1693**	**76**
Shah S.No.35	30.765	0.403	13.627	0.440	3.960	0.946	28.912	0.881	0.194	3.206	0.017	12.127	2.029	1.873	0.570	99.950	65A M18 5	**1656**	**76**

Shah S.No.36	30.686	0.357	13.824	0.344	3.730	0.751	29.186	0.842	0.262	3.314	0.003	12.167	1.971	1.814	0.472	99.721	65A M18 6	**1638**	**84**
Shah S.No.37	31.549	0.352	13.804	0.326	3.570	0.874	29.392	0.799	0.219	3.304	0.008	12.088	2.000	1.814	0.563	100.662	65A M18 7	**1688**	**88**
Shah S.No.38	31.176	0.374	13.824	0.427	3.540	0.879	29.225	0.786	0.191	3.176	0.012	12.049	2.020	1.814	0.516	100.010	65A M18 8	**1677**	**82**
Shah S.No.39	31.314	0.327	14.010	0.357	3.140	0.852	29.627	0.719	0.171	3.314	0.006	12.245	1.951	1.824	0.492	100.348	65A M18 9	**1679**	**92**
Shah S.No.40	31.784	0.327	13.873	0.419	2.970	0.713	29.569	0.683	0.359	3.206	0.007	12.392	2.078	1.794	0.457	100.631	65A M18 10	**1664**	**90**
Monazite within matrix																			
Shah S.No.41	31.804	0.319	14.059	0.390	2.950	1.450	29.167	0.681	0.121	3.314	0.000	12.245	1.971	1.569	0.577	100.617	C75 M1 1	**1668**	**92**
Shah S.No.42	31.686	0.306	14.245	0.333	2.930	1.460	29.108	0.685	0.126	3.363	0.014	12.314	2.020	1.569	0.630	100.787	C75 M1 2	**1685**	**98**
Shah S.No.43	31.784	0.259	14.422	0.271	2.550	1.300	29.784	0.574	0.116	3.431	0.000	12.235	2.020	1.549	0.530	100.825	C75 M1 3	**1671**	**111**
Shah S.No.44	31.706	0.262	14.804	0.297	2.540	1.310	29.657	0.583	0.101	3.284	0.010	12.029	1.931	1.520	0.598	100.633	C75 M1 4	**1655**	**108**
Shah S.No.45	31.578	0.238	14.618	0.271	2.340	1.221	29.471	0.550	0.089	3.304	0.000	12.284	2.118	1.784	0.456	100.321	C75 M1 5	**1635**	**116**
Shah S.No.46	31.461	0.367	13.882	0.534	3.120	1.590	28.716	0.771	0.125	3.225	0.000	12.127	2.020	1.676	0.622	100.237	C75 M1 6	**1658**	**81**
Shah S.No.47	31.676	0.231	14.500	0.277	2.150	1.300	29.735	0.515	0.099	3.333	0.002	12.333	1.931	1.529	0.559	100.171	C75 M1 7	**1669**	**122**
Shah S.No.48	31.265	0.509	13.255	0.648	4.470	1.920	28.029	1.066	0.207	3.196	0.006	11.902	1.941	1.775	0.654	100.844	C108 M4 1	**1699**	**65**
Shah S.No.49	31.343	0.482	13.275	0.603	4.490	1.880	28.127	0.968	0.218	3.235	0.005	11.990	1.941	1.853	0.704	101.116	C108 M4 2	**1650**	**65**
Shah S.No.50	31.853	0.349	13.765	0.390	3.360	1.630	28.853	0.771	0.188	3.255	0.000	12.078	1.922	1.745	0.596	100.754	C108 M4 3	**1668**	**86**
Shah S.No.51	31.431	0.354	13.804	0.351	3.520	1.400	28.980	0.764	0.153	3.343	0.004	12.490	2.118	2.020	0.652	101.383	C108 M4 4	**1683**	**85**
Shah S.No.52	31.343	0.381	13.676	0.350	3.940	1.410	28.529	0.841	0.186	3.255	0.015	12.373	2.078	1.971	0.692	101.040	C108 M4 5	**1668**	**80**
Shah S.No.53	31.412	0.338	13.784	0.351	3.350	1.420	28.588	0.713	0.160	3.284	0.006	12.471	2.088	2.020	0.681	100.665	C108 M4 6	**1668**	**88**
Shah S.No.54	31.549	0.462	13.108	0.328	5.080	1.450	27.667	1.052	0.259	3.206	0.010	12.392	2.118	2.108	0.583	101.372	C108 M4 7	**1681**	**71**
Shah S.No.55	31.510	0.444	13.029	0.326	4.790	1.490	27.490	1.035	0.210	3.176	0.013	12.353	2.206	2.255	0.633	100.960	C108 M4 8	**1693**	**74**
Shah S.No.56	31.706	0.409	13.098	0.319	4.410	1.450	27.931	0.921	0.232	3.186	0.005	12.490	2.206	2.206	0.694	101.263	C108 M4 9	**1678**	**77**
Shah S.No.57	31.716	0.414	13.696	0.333	4.490	1.430	27.863	0.937	0.225	3.147	0.000	12.206	2.127	2.088	0.585	101.258	C108 M4 10	**1660**	**76**
Shah S.No.58	29.86	0.408	13.52	0.486	3.89	1.49	28.47	0.985	0.297	3.17	0.004	11.47	1.96	1.66	0.66	98.331	C77 M5 1	**1651**	**77**
Shah S.No.59	30.41	0.362	14.2	0.370	3.59	1.44	29.08	0.808	0.173	3.21	0.002	11.82	1.98	1.75	0.673	99.872	C77 M5 2	**1677**	**87**
Shah S.No.60	30.2	0.406	13.57	0.462	3.99	1.51	28.21	0.950	0.341	3.12	0	11.67	2.03	1.83	0.681	98.971	C77 M5 3	**1637**	**76**
Shah S.No.61	29.34	0.358	13.9	0.387	3.64	1.43	28.64	0.861	0.739	3.16	0.012	11.59	1.97	1.68	0.640	98.350	C77 M5 4	**1625**	**85**
Shah S.No.62	30.27	0.316	14.2	0.314	2.95	1.33	29.59	0.735	0.251	3.22	0.012	11.77	2.03	1.69	0.621	99.302	C77 M5 5	**1760**	**103**
Shah S.No.63	29.25	0.343	13.78	0.365	3.25	1.37	28.51	0.770	0.375	3.18	0.007	11.51	1.93	1.67	0.656	96.968	C77 M5 6	**1707**	**91**
Shah S.No.64	30.3	0.330	14.06	0.363	3.36	1.58	29	0.821	0.166	3.14	0.003	12.27	2.08	1.82	0.678	99.972	C77 M5 7	**1618**	**89**
Shah S.No.65	30.11	0.451	13.44	0.536	4.27	1.67	28.22	1.065	0.150	3.11	0.011	11.58	2	1.69	0.657	98.963	C77 M5 8	**1657**	**71**
Shah S.No.66	30.07	0.419	14.17	0.512	3.94	1.53	28.64	0.979	0.132	3.09	0.011	11.38	1.87	1.55	0.596	98.891	C77 M5 9	**1653**	**75**
Shah S.No.67	30.36	0.453	13.17	0.528	4.29	1.77	28.02	1.020	0.144	3.18	0.005	11.85	2.07	1.88	0.741	99.484	C77 M5 10	**1666**	**71**
Shah S.No.68	30.25	0.419	13.67	0.447	4.02	1.62	28.39	0.921	0.167	3.18	0	11.84	1.99	1.8	0.656	99.372	C77 M5 11	**1694**	**78**
Shah S.No.69	30.28	0.568	13.07	0.606	5.38	1.85	27.02	1.238	0.208	3.02	0.019	11.54	2.01	1.87	0.810	99.492	C77 M5 12	**1707**	**62**

Table 6. *(Continued)*

Shah S.No.	P_2O_5	PbO	La_2O_3	UO_2	ThO_2	Y_2O_3	Ce_2O_3	CaO	SiO_2	Pr_2O_3	SO_3	Nd_2O_3	Sm_2O_3	Gd_2O_3	Dy_2O_3	Total	Sample[a]	Age	Error
Shah S.No.70	30.22	0.464	13.57	0.423	4.67	1.52	28.34	0.999	0.243	3.16	0.015	11.54	1.97	1.64	0.655	99.431	C77 M5 13	**1705**	**72**
Shah S.No.71	30.33	0.424	13.85	0.352	4.43	1.44	28.67	0.929	0.209	3.12	0.011	11.71	1.89	1.69	0.616	99.673	C77 M5 14	**1695**	**78**
Shah S.No.72	30.31	0.382	14.03	0.399	3.77	1.49	28.6	0.852	0.166	3.13	0	11.79	2.02	1.8	0.684	99.425	C77 M5 15	**1674**	**83**
Shah S.No.73	30.19	0.485	13.46	0.532	4.58	1.67	27.95	1.052	0.181	3.13	0.004	11.54	1.99	1.8	0.721	99.288	C77 M5 16	**1698**	**69**
Shah S.No.74	30.53	0.491	13.6	0.551	4.67	1.69	28.33	1.093	0.207	3.13	0	11.94	1.98	1.78	0.753	100.746	C77 M5 17	**1681**	**68**
Shah S.No.75	30.45	0.352	13.9	0.335	3.58	1.43	28.77	0.82	0.250	3.2	0.010	12.05	1.89	1.65	0.626	99.316	C83 M6 1	**1675**	**89**
Shah S.No.76	30.5	0.301	14.36	0.290	2.97	1.41	29.79	0.703	0.138	3.33	0.012	12.27	1.91	1.73	0.647	100.364	C83 M6 2	**1708**	**104**
Shah S.No.77	30.33	0.344	14.22	0.317	3.44	1.38	29.34	0.790	0.161	3.22	0.004	12.16	1.9	1.68	0.617	99.905	C83 M6 3	**1708**	**94**
Shah S.No.78	30.03	0.351	14.25	0.363	3.59	1.39	29.27	0.813	0.167	3.22	0.005	11.72	1.79	1.71	0.696	99.397	C83 M6 4	**1636**	**86**
Shah S.No.79	30.33	0.356	14.16	0.342	3.58	1.42	29.22	0.799	0.183	3.23	0	11.78	1.89	1.74	0.669	99.701	C83 M6 5	**1686**	**89**
Shah S.No.80	30.39	0.381	14.02	0.386	3.68	1.48	29.05	0.876	0.159	3.22	0.020	11.99	1.98	1.75	0.652	100.036	C83 M6 6	**1711**	**85**
Shah S.No.81	30.35	0.448	13.57	0.485	4.26	1.67	28.22	1.001	0.146	3.16	0.007	11.74	1.97	1.84	0.798	99.666	C83 M6 7	**1696**	**74**
Shah S.No.82	30.3	0.351	14.17	0.392	3.43	1.5	28.96	0.829	0.134	3.2	0.013	11.84	1.91	1.76	0.701	99.493	C83 M6 8	**1655**	**87**
Shah S.No.83	30.25	0.402	14.03	0.428	3.86	1.58	28.47	0.916	0.138	3.16	0.008	11.78	1.92	1.7	0.684	99.328	C83 M6 9	**1693**	**81**
Shah S.No.84	30.765	0.604	12.382	0.424	6.930	1.193	26.598	1.588	0.393	2.941	0.021	11.333	2.069	2.265	0.641	100.149	65A M10 1	**1631**	**56**
Shah S.No.85	31.245	0.501	13.147	0.276	5.670	1.053	27.608	1.195	0.362	3.049	0.015	11.667	2.049	2.098	0.562	100.497	65A M10 2	**1712**	**68**
Shah S.No.86	30.618	0.422	13.363	0.424	4.350	0.955	28.559	0.976	0.218	3.196	0.008	12.020	2.059	1.951	0.542	99.660	65A M10 3	**1638**	**73**
Shah S.No.87	31.216	0.417	13.343	0.450	3.980	0.934	29.020	0.871	0.218	3.118	0.013	12.059	2.078	1.961	0.544	100.220	65A M10 4	**1693**	**76**
Shah S.No.88	30.765	0.403	13.627	0.440	3.960	0.946	28.912	0.881	0.194	3.206	0.017	12.127	2.029	1.873	0.570	99.950	65A M10 5	**1656**	**76**
Shah S.No.89	30.686	0.357	13.824	0.344	3.730	0.751	29.186	0.842	0.262	3.314	0.003	12.167	1.971	1.814	0.472	99.721	65A M10 6	**1638**	**84**
Shah S.No.90	31.549	0.352	13.804	0.326	3.570	0.874	29.392	0.799	0.219	3.304	0.008	12.088	2.000	1.814	0.563	100.662	65A M10 7	**1688**	**88**
Shah S.No.91	31.176	0.374	13.824	0.427	3.540	0.879	29.225	0.786	0.191	3.176	0.012	12.049	2.020	1.814	0.516	100.010	65A M10 8	**1677**	**82**
Shah S.No.92	31.314	0.327	14.010	0.357	3.140	0.852	29.627	0.719	0.171	3.314	0.006	12.245	1.951	1.824	0.492	100.348	65A M10 9	**1679**	**92**
Shah S.No.93	31.784	0.327	13.873	0.419	2.970	0.713	29.569	0.683	0.359	3.206	0.007	12.392	2.078	1.794	0.457	100.631	65A M10 10	**1664**	**90**
Shah S.No.94	31.520	0.284	13.980	0.310	2.680	1.229	29.578	0.647	0.117	3.255	0.019	12.245	2.010	1.971	0.662	100.508	65A M11 9	**1699**	**106**
Shah S.No.95	31.235	0.247	13.922	0.283	2.340	1.240	29.804	0.573	0.231	3.235	0.017	12.324	2.049	2.020	0.679	100.198	65A M11 10	**1671**	**115**
Shah S.No.96	31.500	0.245	13.902	0.276	2.320	1.162	30.186	0.549	0.131	3.294	0.006	12.706	2.118	1.971	0.632	100.997	65A M11 11	**1682**	**117**
Shah S.No.97	31.088	0.225	14.098	0.263	2.200	1.120	29.882	0.540	0.129	3.314	0.015	12.480	2.010	1.912	0.702	99.977	65A M11 12	**1629**	**121**
Shah S.No.98	31.431	0.219	14.265	0.299	1.890	0.758	30.549	0.465	0.078	3.343	0.007	12.608	2.010	1.716	0.494	100.131	65A M11 13	**1677**	**128**
Shah S.No.99	30.500	0.217	15.000	0.327	1.840	0.441	30.961	0.484	0.089	3.412	0.013	12.333	1.980	1.520	0.414	99.530	65A M11 14	**1639**	**126**

[a] Sample number, porphyroblast and monazite.

Table 7. *Complete data about the chemical analyses of all monazite grains, preserved within porphyroblasts and matrix phases of samples aligned to FIA set 4.*

Shah S.No.	P_2O_5	PbO	La_2O_3	UO_2	ThO_2	Y_2O_3	Ce_2O_3	CaO	SiO_2	Pr_2O_3	SO_3	Nd_2O_3	Sm_2O_3	Gd_2O_3	Dy_2O_3	Total	Sample[a]	Age	Error
Monazite within porphyroblast																			
Shah S.No.1	30.220	0.489	13.040	0.211	7.180	1.128	26.660	1.285	0.491	3.050	0.000	12.060	2.040	1.560	0.539	99.953	C51B Crd M19 1	**1419**	**56**
Shah S.No.2	30.040	0.349	13.090	0.211	4.950	1.130	26.830	1.059	2.390	3.170	0.012	12.230	2.120	1.620	0.508	99.708	C51B Crd M19 2	**1407**	**72**
Shah S.No.3	30.080	0.342	13.470	0.188	4.910	1.089	27.540	0.952	0.323	3.310	0.000	12.590	2.120	1.720	0.551	99.186	C51B Crd M19 3	**1412**	**74**
Shah S.No.4	30.200	0.344	13.570	0.185	4.720	1.047	27.890	0.937	0.492	3.220	0.018	12.480	2.030	1.620	0.470	99.222	C51B Crd M19 4	**1470**	**77**
Shah S.No.5	30.290	0.313	14.010	0.204	4.510	1.083	28.030	0.906	0.261	3.260	0.006	12.730	2.130	1.670	0.469	99.872	C51B Crd M19 5	**1378**	**77**
Shah S.No.6	30.390	0.302	14.190	0.206	4.360	1.090	28.570	0.821	0.263	3.270	0.010	12.740	2.090	1.660	0.549	100.511	C51B Crd M19 6	**1366**	**78**
Shah S.No.7	30.510	0.317	13.810	0.207	4.220	1.120	28.350	0.883	0.272	3.250	0.012	12.750	2.140	1.670	0.541	100.050	C51B Crd M19 7	**1466**	**82**
Shah S.No.8	30.360	0.305	13.720	0.209	4.200	1.086	28.320	0.841	0.269	3.370	0.015	12.730	2.130	1.660	0.508	99.723	C51B Crd M19 8	**1419**	**81**
Shah S.No.9	30.730	0.294	13.840	0.209	3.880	1.083	28.190	0.791	1.972	3.320	0.003	12.440	2.110	1.630	0.445	100.937	C51B Crd M19 9	**1459**	**87**
Shah S.No.10	30.580	0.242	14.470	0.206	3.280	1.121	28.890	0.669	0.244	3.330	0.000	12.730	2.110	1.610	0.515	99.997	C51B Crd M19 10	**1386**	**96**
Shah S.No.11	30.610	0.230	14.410	0.190	2.960	1.130	29.500	0.625	0.160	3.350	0.007	12.740	2.230	1.680	0.574	100.394	C51B Crd M19 11	**1451**	**107**
Shah S.No.12	30.430	0.191	14.430	0.200	2.540	1.136	29.800	0.537	0.153	3.450	0.018	13.430	2.240	1.750	0.516	100.822	C51B Crd M19 12	**1356**	**114**
Shah S.No.13	30.530	0.174	14.640	0.187	2.340	1.088	29.540	0.508	0.131	3.380	0.000	12.900	2.150	1.620	0.541	99.729	C51B Crd M19 13	**1338**	**123**
Shah S.No.14	30.660	0.360	13.360	0.264	5.060	1.213	26.880	1.018	0.318	3.190	0.018	12.190	2.040	1.660	0.634	98.864	C77 Crd M20 1	**1381**	**69**
Shah S.No.15	30.220	0.365	13.620	0.227	5.060	1.087	27.770	0.964	0.296	3.190	0.000	12.200	2.060	1.630	0.569	99.258	C77 Crd M20 2	**1430**	**71**
Shah S.No.16	30.510	0.372	13.440	0.283	4.990	1.209	27.340	1.006	0.221	3.220	0.002	12.440	2.060	1.790	0.504	99.387	C77 Crd M20 3	**1427**	**70**
Shah S.No.17	30.960	0.304	13.990	0.204	4.260	1.026	28.150	0.850	0.222	3.280	0.009	12.440	1.930	1.520	0.554	99.699	C77 Crd M20 4	**1405**	**81**
Shah S.No.18	30.830	0.297	13.510	0.237	4.050	1.191	27.860	0.815	0.193	3.310	0.002	12.590	2.080	1.720	0.527	99.212	C77 Crd M20 5	**1397**	**82**
Shah S.No.19	30.870	0.284	14.130	0.198	3.910	1.152	28.040	0.806	0.188	3.290	0.007	12.400	1.970	1.700	0.477	99.421	C77 Crd M20 6	**1418**	**87**
Shah S.No.20	30.830	0.276	14.190	0.235	3.700	1.152	28.180	0.773	0.160	3.240	0.007	12.290	2.030	1.690	0.574	99.328	C77 Crd M20 7	**1401**	**86**
Shah S.No.21	30.860	0.265	14.220	0.197	3.530	1.108	28.380	0.743	0.177	3.260	0.015	12.540	2.010	1.700	0.559	99.563	C77 Crd M20 8	**1437**	**93**
Shah S.No.22	30.860	0.242	13.940	0.194	3.310	1.080	28.460	0.678	0.157	3.350	0.001	13.180	2.090	1.750	0.527	99.818	C77 Crd M20 9	**1390**	**97**
Shah S.No.23	30.260	0.224	14.060	0.189	2.990	1.121	29.110	0.700	0.188	3.360	0.007	12.910	2.280	1.710	0.562	99.671	C77 Crd M20 10	**1409**	**104**
Shah S.No.24	30.340	0.370	13.470	0.537	3.960	1.560	28.350	0.972	0.200	3.160	0.002	12.180	2.110	1.770	0.697	99.678	C110 And M21 1	**1448**	**71**
Shah S.No.25	30.590	0.299	13.830	0.384	3.460	1.390	29.350	0.797	0.208	3.310	0.006	12.450	2.070	1.690	0.615	100.449	C110 And M21 2	**1425**	**82**
Shah S.No.26	30.540	0.288	14.040	0.406	3.180	1.420	29.640	0.749	0.158	3.320	0.005	12.620	2.140	1.710	0.687	100.904	C110 And M21 3	**1434**	**86**
Shah S.No.27	30.560	0.213	14.210	0.289	2.600	1.244	29.960	0.603	0.274	3.310	0.000	12.600	2.080	1.660	0.583	100.186	C110 And M21 4	**1353**	**104**
Shah S.No.28	30.340	0.227	14.060	0.288	2.470	1.228	30.040	0.578	0.100	3.320	0.010	12.790	2.070	1.640	0.623	99.784	C110 And M21 5	**1489**	**110**

Table 7. *(Continued)*

Shah S.No.	P_2O_5	PbO	La_2O_3	UO_2	ThO_2	Y_2O_3	Ce_2O_3	CaO	SiO_2	Pr_2O_3	SO_3	Nd_2O_3	Sm_2O_3	Gd_2O_3	Dy_2O_3	Total	Sample[a]	Age	Error
Monazite within matrix																			
Shah S.No.29	31.14	0.296	13.64	0.351	3.33	1.41	29.08	0.794	0.326	3.27	0.002	12.3	2.12	1.71	0.613	100.384	C110 M9 1	**1482**	**88**
Shah S.No.30	30.77	0.243	13.93	0.372	2.51	1.43	29.52	0.596	0.139	3.34	0.011	12.69	2.13	1.68	0.635	99.998	C110 M9 2	**1458**	**100**
Shah S.No.31	30.79	0.310	13.71	0.389	3.6	1.4	29.16	0.810	0.157	3.23	0.015	12.55	2.09	1.66	0.641	100.515	C110 M9 3	**1432**	**80**
Shah S.No.32	31.38	0.209	14.14	0.282	2.23	1.28	30.12	0.557	0.209	3.33	0.007	12.59	2.12	1.65	0.630	100.737	C110 M9 4	**1483**	**117**
Shah S.No.33	31.14	0.235	13.99	0.323	2.54	1.27	29.88	0.593	0.262	3.36	0.000	12.72	2.13	1.64	0.578	100.663	C110 M9 5	**1461**	**104**
Shah S.No.34	30.89	0.464	12.66	0.692	5.05	1.79	27.09	1.231	0.276	3.1	0.000	11.85	2.09	1.77	0.758	99.713	C110 M9 6	**1423**	**57**
Shah S.No.35	31.13	0.434	12.51	0.623	4.87	1.85	26.81	1.135	0.372	3.09	0	11.94	2.15	1.84	0.733	99.489	C110 M9 7	**1410**	**59**

[a] Sample number, porphyroblast and monazite.

foliation gave an age of 1762 ± 35 Ma (figure 9). This sample preserves FIA sets 1 and 2 within staurolite porphyroblasts (figure 8). The monazite grains are not zoned (figures 10 and 11).

5.3 *Sample C84 (FIA 2 in garnet and 3 in staurolite)*

The dominant foliation in the matrix (S_{e1}) contains a single monazite grain that lies sub-parallel to it that has an age of 1729 ± 23 Ma (see tables 3 and 5).

5.4 *Sample C65A (FIA 1 in garnet and 2 plus FIA 3 in staurolite)*

Two monazite grains in the main matrix foliation (S_{ea}) have ages 1742 ± 29 Ma and 1665 ± 23 Ma (e.g., table 3; figures 12 and 13). Both lie sub-parallel to S_{ea}. A monazite grain in staurolite is shown in figure 14).

5.5 *Sample C43 (FIA 1 in garnet and 2 in staurolite)*

A single monazite grain parallel to the main matrix foliation (S_{e1}) has an age of 1724 ± 37 Ma (see tables 3 and 5). This sample preserves FIA sets 1 and 2 within garnet and staurolite porphyroblasts.

5.6 *Sample C51B (FIA 3 in cordierite)*

A single monazite grain lying orthogonal to the main matrix foliation (S_{e1}) in this sample has an age of 1685 ± 29 Ma (see tables 3 and 6). This sample preserves FIA set 3 within cordierite porphyroblasts.

5.7 *Sample C77 (FIA 3 in cordierite)*

A single monazite grain lying in the youngest matrix foliation (S_{e3}) in this sample has an age of 1677 ± 19 Ma (see tables 3 and 6). This sample preserves FIA set 3 within cordierite porphyroblasts.

5.8 *Sample C108 (FIA 1 in garnet and 2 in staurolite)*

A single monazite grain sub-parallel to the main matrix foliation (S_{e1}) has an age of 1675 ± 24 Ma (see tables 3 and 6). This sample preserves FIA sets 1 and 2 within garnet and staurolite porphyroblasts.

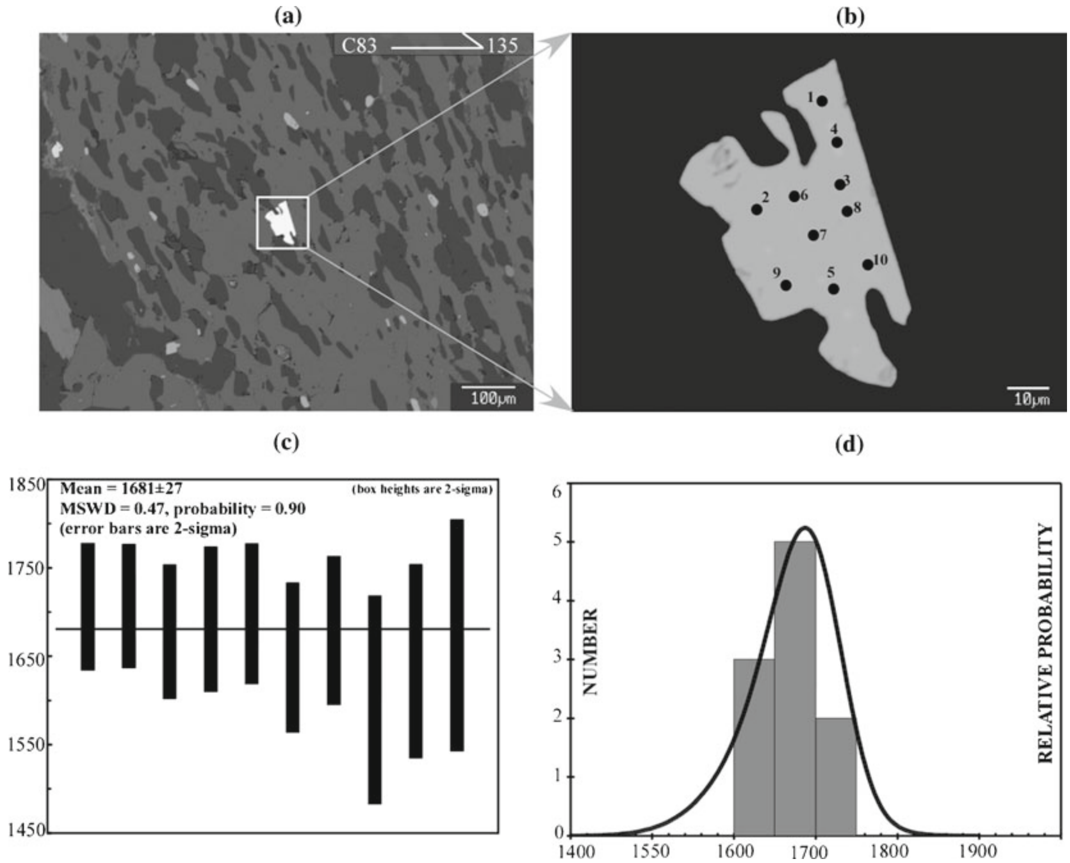

Figure 7. (**a**) Back scatter image shows the staurolite porphyroblast, which contains a single monazite grain lying parallel to the orientation of the foliation. A mean age of 1681 ± 27 Ma is dated from a total of 10 spots analyzed (Sanislav and Shah 2010). (**b**) Enlarged view of the monazite grain with black spots showing the location of each analysis. In (**c**) the weighted average age plot is shown, created by using Isoplot software (Ludwig 1998) and (**d**) is showing the probability density plot.

5.9 *Sample C110 (FIA 4 in andalusite)*

A single monazite grain sub-parallel to the main matrix foliation (S_{e1}) has an age of 1438 ± 30 Ma (see tables 3 and 7). This sample preserves FIA set 4 within andalusite porphyroblasts.

6. Compositional mapping of monazite grains

Samples containing monazite were compositionally mapped for Th, Y, U, Pb and Ce using the JEOL JXA-8300 Superprobe. Most were devoid of any apparent chemical zoning (e.g., figures 10 and 11). One monazite in the matrix of sample C65A showed chemical zoning in both Th and Y (figure 13). Dating of 1742 ± 29 and 1668 ± 48 Ma suggests that this was a product of FIAs 1 and 3 (see below). Sample C75 showed a single example of a monazite with slight zoning in Th preserved within a staurolite porphyroblast (figure 11). A mean age of 1712 ± 25 Ma was analyzed from this grain.

7. Interpretation and discussion

7.1 *The ages within porphyroblast containing FIAs*

The monazite grains stored within foliations defining FIAs in garnet, staurolite (Sanislav and Shah 2010), cordierite and andalusite have recorded ages over an extended period of metamorphism. For example garnet in sample C117, preserves the oldest deformation event recorded in the area at 1756 ± 22 Ma. The date obtained from this porphyroblast agrees with the other samples containing the same FIA sets. This is shown in sample C84, which records the same event in garnet at 1762 ± 21 Ma and fits well with its FIA. The younger grain stored within staurolite is ellipsoidal and aligned parallel to the foliation defined by the inclusion trails and should give a representative age for FIA 3 (Sanislav and Shah 2010). The 1666 ± 26 Ma age in garnet (C51B) accords with the dates obtained from other samples bearing this FIA set (e.g., staurolite grains dated in Sanislav and Shah 2010). The two dates obtained from monazite grains preserved within pseudo-FIA in cordierite (set 3) and as

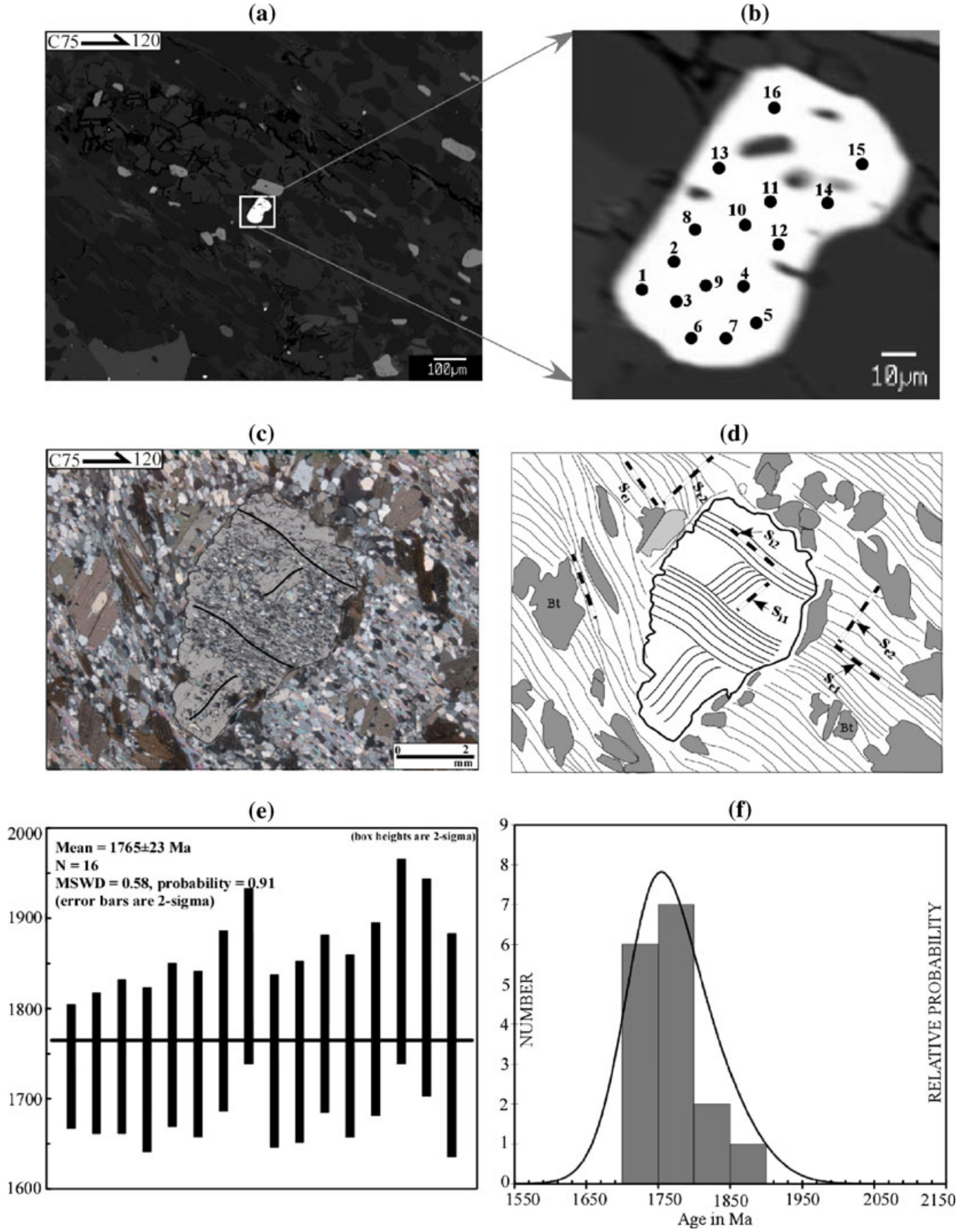

Figure 8. (**a**) Back scatter electron image shows a staurolite porphyroblast, which preserves a single euhedral monazite grain lying orthogonal to the orientation of the foliation. A mean age of 1765 ± 23 Ma is dated from a total of 16 spots analyzed (Sanislav and Shah 2010). (**b**) Enlarged view of the monazite grain with black spots showing the location of each analysis. X-ray images of this monazite grain are shown in this figure. (**c**) Orientated photomicrograph displays the larger view of the staurolite dated. Two different foliations are preserved within staurolite porphyroblast. Monazite grain was contained within a crenulation cleavage. In this sample, staurolite contains a pseudo-FIA belonging to set 1 FIA plus FIA set 2. Thin section is vertical, the light is plane-polarized and single barbed arrow indicates way up and strike. (**d**) Line diagram, shows the detailed features preserved. In (**e**) weighted average age plot is shown which is created by using Isoplot software (Ludwig 1998) and in (**f**) the probability density plot is shown. Se: external foliation, Si: internal foliation, Grt: garnet, St: staurolite, and Bt: Biotite.

single FIA in andalusite (set 3) in the sample C77, accord with the dates obtained from other samples for this event (table 3). The two earlier ages acquired from monazite grains within the main foliation of cordierite are relics of an older foliation that lies oblique to the main foliation defined by the

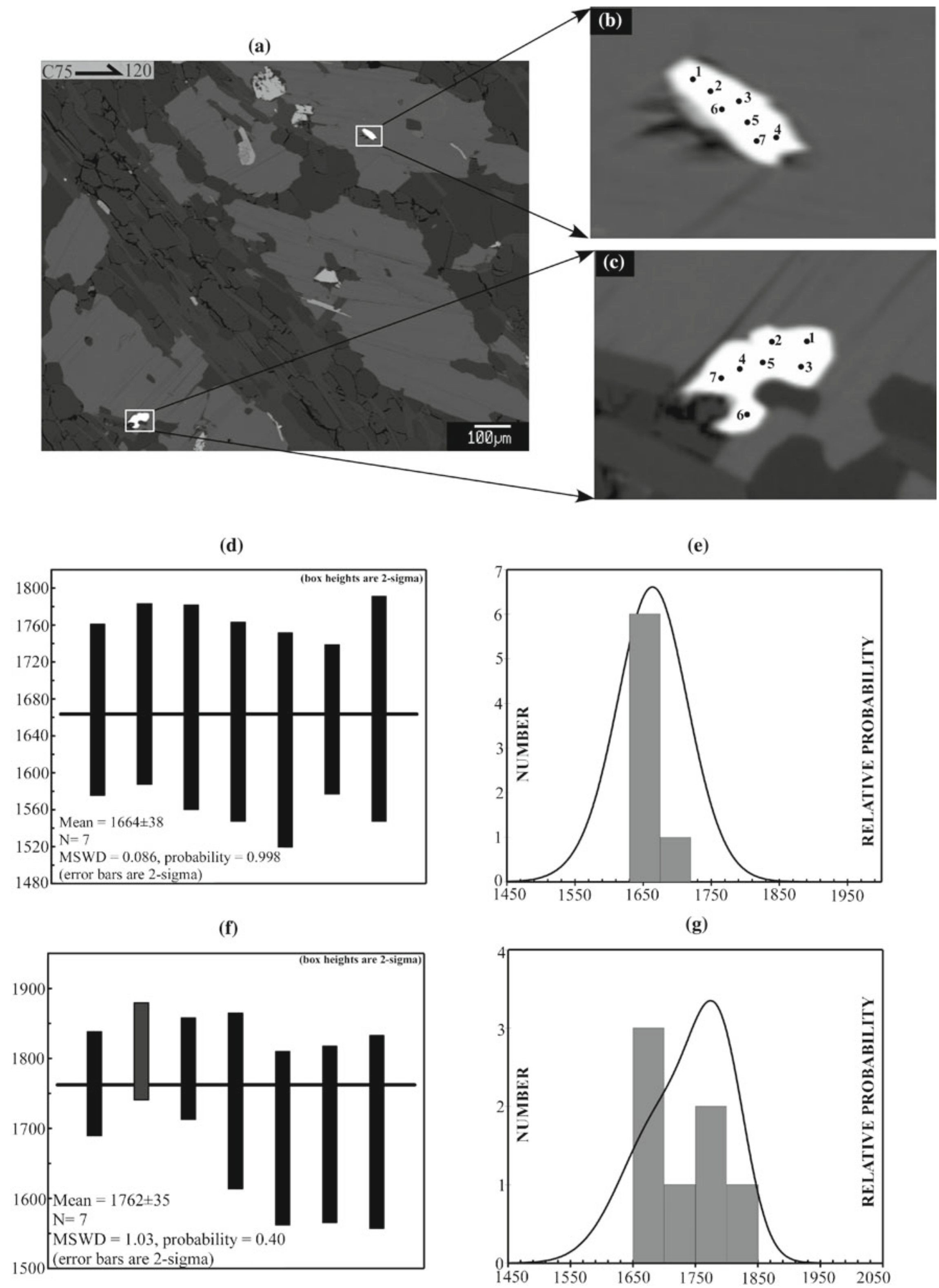

Figure 9. (**a**) Back scatter electron image shows two monazite grains preserved within matrix foliation of sample C75. (**b**) Enlarged view of a monazite grain with black spots showing the location of each analysis. This euhedral grain is preserved within the main matrix foliation and is located parallel to its orientation. A mean age of 1664 ± 38 Ma is dated from a total of seven spots analyzed. (**c**) Enlarged view of a monazite grain with black spots showing the location of each analysis. This grain is oriented orthogonal to the orientation of the main matrix foliation. A mean age of 1762 ± 35 Ma is dated from a total of seven spots analyzed. Thin section is vertical, single barbed arrow indicates way up and strike. In (**d** and **f**) weighted average age plots are shown, created by using Isoplot software (Ludwig 1998) and in (**e** and **g**) the probability density plots are shown.

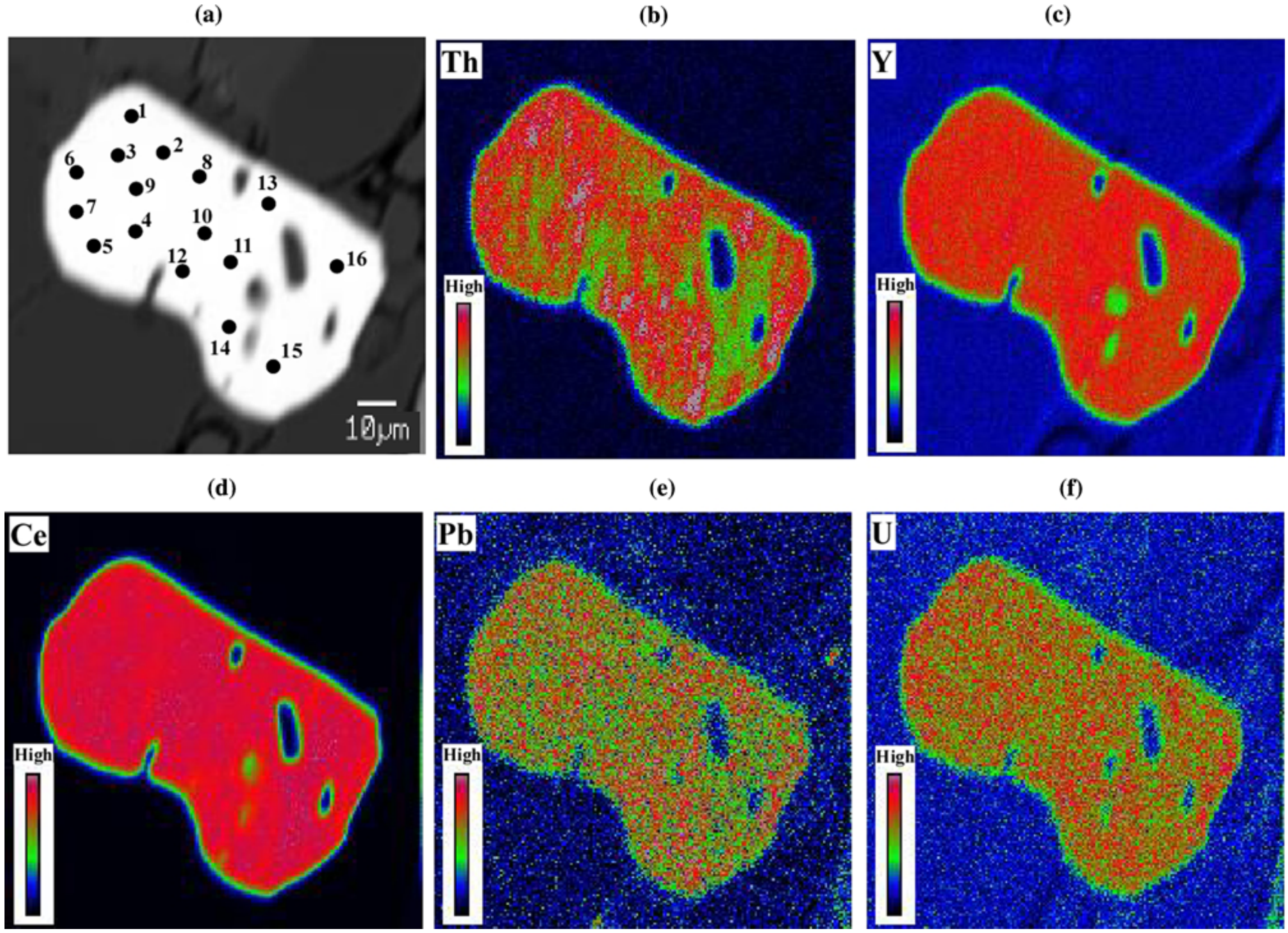

Figure 10. (**a**) Back scatter oriented electron image of a monazite grain preserved within the foliation of porphyroblast that contains the inclusion trails of FIA set 1 in sample (C75). The location of each analysis is shown by black spots. In (**b**) through (**f**), X-ray maps of Th, Y, Ce, Pb and U are shown. Chemical zoning in Th and Pb is crudely present.

inclusion trails. Their dates are compatible with the ages obtained from FIA sets 1 and 2, preserved within other samples. The date acquired from two monazites in cordierite (C51B) accords with the dates obtained from other samples for FIA set 4 (see table 3). An older age within this sample from one monazite is consistent with an earlier foliation aligned to FIA set 1 and represents its relics. The age recorded in sample C110 is consistent with the youngest FIA set observed.

7.2 *Combining the age data within FIA sets*

Monazite grains are common within staurolite (Sanislav and Shah 2010), cordierite and andalusite porphyroblasts but rare in garnet. Of the 11 samples investigated, five contained inclusion trails defining FIA set 1; six monazite grains were identified and 93 analyses completed defining an age of 1760.5 ± 9.7 Ma (table 3; figure 15a and b). Five samples contained inclusion trails defining FIA set 2; eight monazite grains were identified and 136 analyses completed defining an age of 1719.7 ± 6.4 Ma (table 3; figure 15c and d). Five samples contained inclusion trails defining FIA set 3; five monazite grains were identified and 56 analyses completed defining an age of 1674 ± 11 Ma (table 3; figure 15e and f). Three samples contained inclusion trails defining FIA set 4; three monazite grains were identified and 28 analyses completed defining an age of 1415 ± 16 Ma (table 3; figure 15g and h). These ages (1760.5 ± 9.7, 1719.7 ± 6.4, 1674 ± 11 and 1415 ± 16 Ma), respectively, confirm the FIA 1, 2, 3, 4 succession established using core/rim criteria plus the previously recognized (Tweto 1987; Nyman *et al.* 1994; Karlstrom *et al.* 1997) separation of orogenesis into two distinct periods 250 million years apart (Shah 2010).

7.3 *The significance of FIAs for determining monazite ages*

Texturally controlled dating of monazite inclusions has recently been used by many petrologists

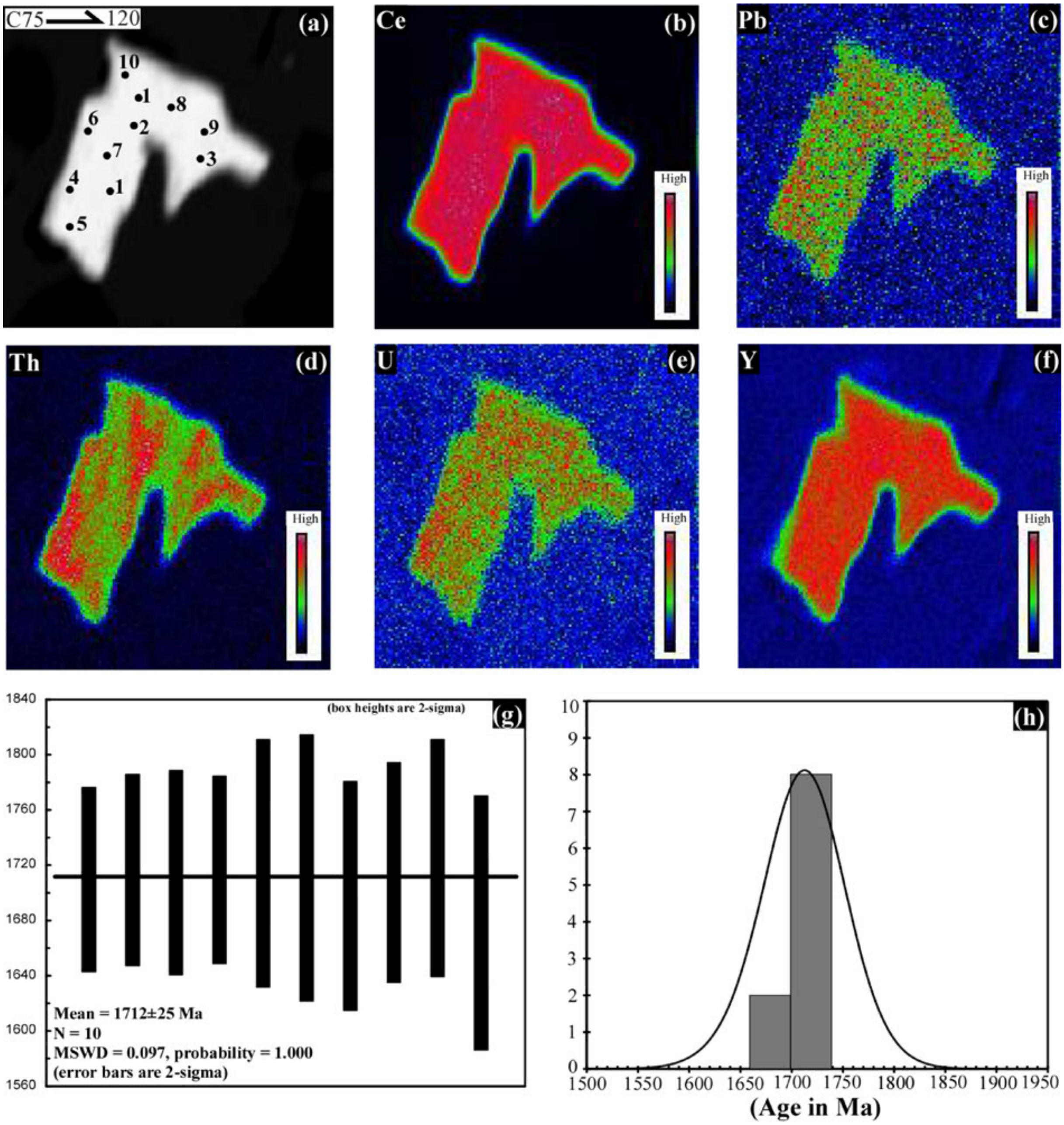

Figure 11. (**a**) Back scatter oriented electron image of a monazite grain preserved within the foliation of porphyroblast that contains the inclusion trails of FIA set 2, in sample (C75). The location of each analysis is shown by black spots. Single barbed arrow indicates way up and strike. In (**b**) through (**f**) X-ray maps of Ce, Pb, Th, U and Y are shown. Chemical zoning in Th is crudely present. A single mean age of 1712 ± 25 Ma is preserved within this monazite, which is coeval with the ages obtained from the other samples for the regional deformation that produced this FIA set. In (**g**) the weighted average age plot of eight spots is shown which is created by using Isoplot software (Ludwig 1998) and in (**h**) the probability density plot is shown.

around the world to date foliation ages (Williams *et al.* 1999; Shaw *et al.* 2001; Dahl *et al.* 2005). A range of ages will always be present in the matrix due to the potential for the preservation of monazite grains within the strain shadows of successively grown porphyroblasts and this is exemplified by table 3. Depending on the timing of porphyroblast growth, a similar range can be preserved from the influence of younger events. The most critical phase in using an absolute microstructural dating method is to accurately identify monazite grains within a particular textural and structural setting. FIA provide such a setting and offer a robust opportunity to extract *in situ* information from individual monazite grains preserved within an independently determined relative timeframe.

The accord between FIA set and age recorded herein is remarkable (table 3). Only one sample

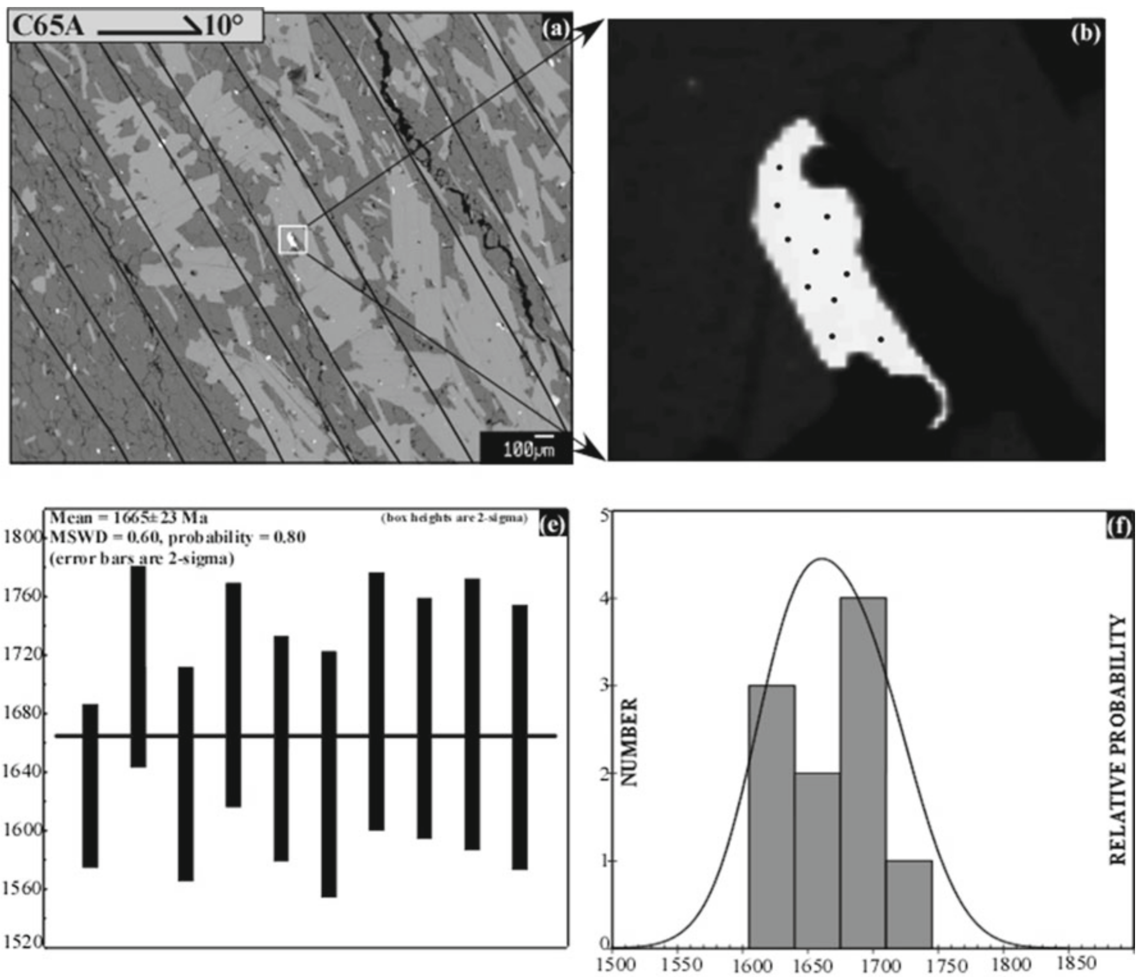

Figure 12. (**a**) Shows a back scatter in which a monazite grain is preserved within a matrix foliation which is lying parallel to the orientation of the foliation. A mean age of 1665 ± 23 Ma is dated from a total of 10 spots analyzed. (**b**) Enlarged view of the monazite grain with black spots showing the location of each analysis. Single barbed arrow indicates way up and strike. In (**e**) the weighted average age plot of 18 spots is shown, created by using Isoplot software (Ludwig 1998). (**f**) shows a probability density plot.

(C77) contains 'anomalous' older ages which can be attributed to the earlier events as just mentioned. The recognition of pseudo-FIAs and FIAs provided tight control over what FIA sets were preserved in each sample. Without this level of control on the distribution of FIAs, the ∼100 million year range in ages obtained (not including the far younger ∼1400 Ma ages) would have been attributed to noise. Instead it accords perfectly with the independently obtained succession of FIA sets!

7.4 *The ages within matrix*

The older monazite grain (1762 ± 35 Ma) in sample C75, accords with the dates acquired for FIA set 1 (table 3). The younger matrix age obtained is coeval with dates acquired for FIA set 3 suggesting that the matrix was reused or reactivated during the development of this FIA set. The single matrix age in sample (C84), accords with the date for FIA set 2 (table 3) and is interpreted to represent a relic of an earlier-formed foliation. Similar ages were obtained within the sample C65A, which are consistent FIA sets 1 and 3 (table 3) and are interpreted to represent relics of earlier-formed foliations preserved within the strain shadows of porphyroblast. In sample C43, the matrix age obtained (1724 ± 37 Ma) accords with the dates acquired for FIA set 2 (see table 3), which suggests reactivation of the matrix during these events. This monazite grain was parallel to the main matrix foliation (S_{e1}). Another relic age (1723 ± 34 Ma) was acquired in the sample C83, and is consistent with FIA set 2 rather than for FIA set 3. This suggests that this grain was not deformed and recrystallized during the development of FIA 3 prior to staurolite growth. Some crystallographic orientations of grains relative to a developing strain field can make

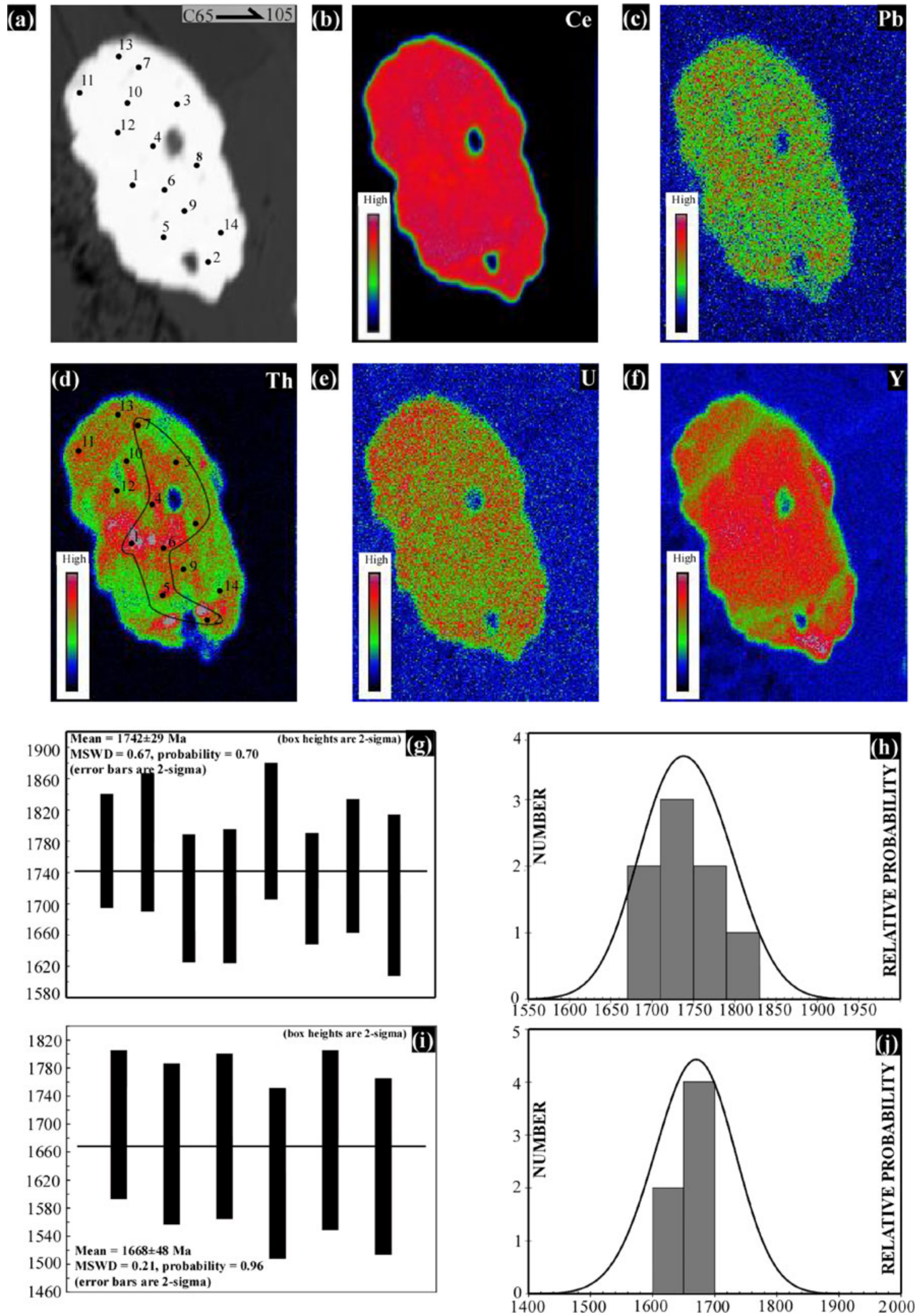

Figure 13. (**a**) Back scatter oriented electron image of a monazite grain preserved within the matrix of the sample (C65A), which shows the location of each analysis. (**b**) through (**f**), shows the X-ray maps of Ce, Pb, Th, U and Y respectively. Age zoning in the chemical contents of Th and Y is present, which offer two different age domains. A mean age of 1742 ± 29 Ma is preserved within high Th domains (polygonal area). The relatively low Th regions contain a mean age of 1668 ± 48 Ma. Thin section is vertical, single barbed arrow indicates way up and strike. (**g** and **i**) shows weighted average age plots, created by using Isoplot software (Ludwig 1998) and in (**h** and **j**) the probability density plot is shown.

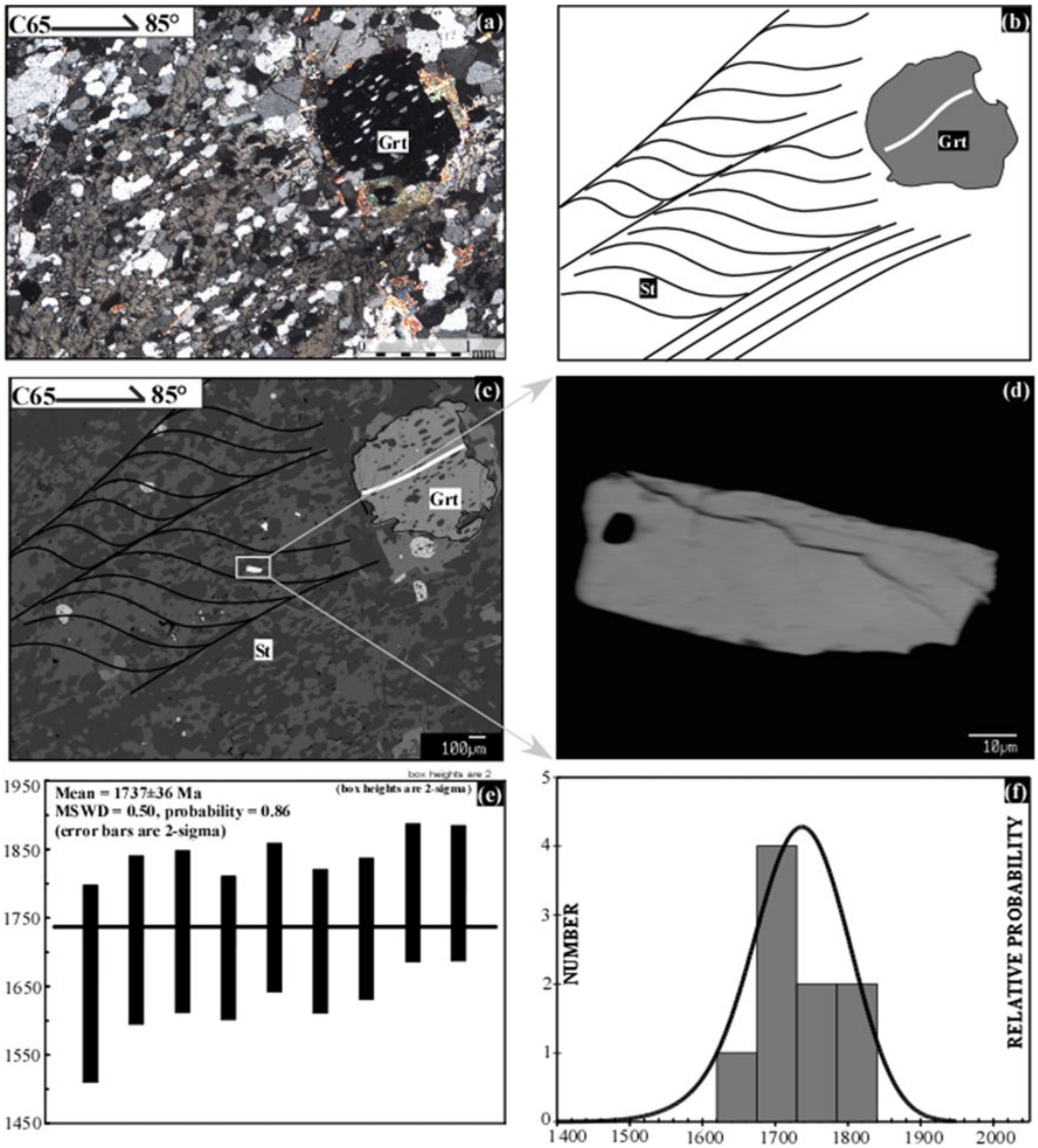

Figure 14. (**a** and **b**) Photomicrograph and accompanying line diagram from sample C65A (cross polarized light) which preserves a crenulated and a crenulation cleavage within staurolite porphyroblast. Garnet also contains a foliation which is different from those contained within the staurolite. Thin section is vertical, the light is cross-polarized and the single barbed arrow indicates way up and strike. (**b**) Back scatter image shows the staurolite porphyroblast preserving a single euhedral monazite grain within a crenulated cleavage of the same thin section. A mean age of 1737 ± 36 Ma is dated from a total of nine spots analyzed (Sanislav and Shah 2010). (**c**) Enlarged view of the monazite. In (**e**) weighted average age plot of 18 spots is shown which is created by using Isoplot software (Ludwig 1998) and (**f**) shows the probability density plot.

a particular mineral phase very competent and hard to deform (e.g., Mancktelow 1981). This grain could reflect such a phenomenon. In samples C51B, C77 and C108, the acquired ages accord with the dates obtained for FIA set 3 suggesting these monazites grew at this time and were preserved through modification of the matrix by subsequent deformation events. A younger age was preserved within a monazite of sample C110, which is consistent with ages for FIA set 4. This was obtained in the foliations preserved within the andalusite porphyroblast, which are very similar to and continuous with the matrix.

7.5 *Assessing the spread of the age data from matrix relative to that for the FIA succession*

Monazite grains are common within the matrix and randomly distributed. They are generally preserved

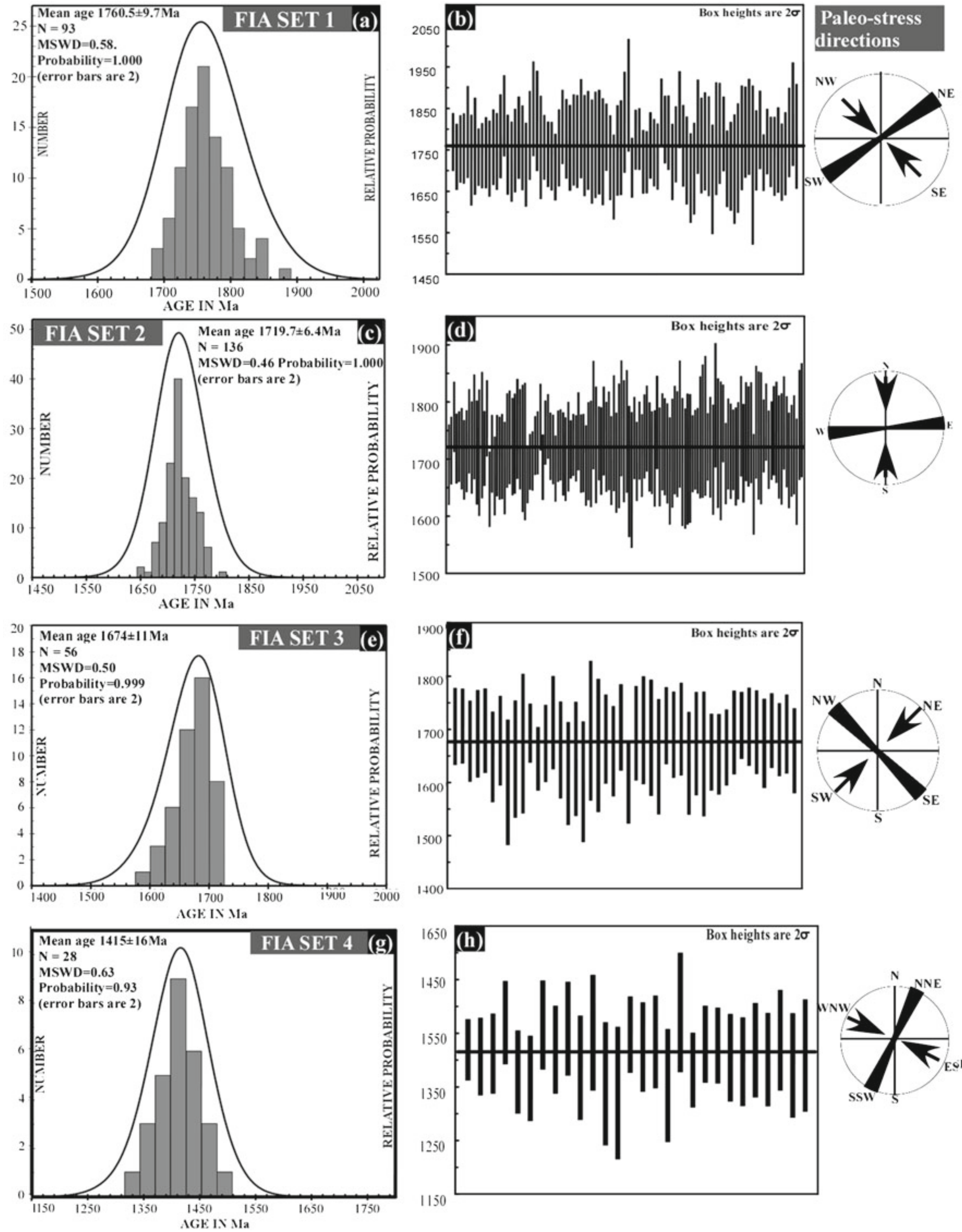

Figure 15. Probability density and weighted average age plots (**a**–**h**) for all samples in which monazite grains were dated within matrix. These plots were created in Isoplot software (Ludwig 1998). Complete chemical data is shown in tables 4–7.

within muscovite and biotite grains (e.g., figures 9 and 12). A total of nine samples out of 30 investigated contained monazite crystals in the matrix. Two samples each contain a monazite grain, from which a total of 14 analyses were completed defining an age of 1749 ± 23 Ma (table 3; figure 16a and b). Four samples contained four monazite grains from which 28 analyses were obtained defining an age of 1726 ± 17 Ma (table 3; figure 16c and d). Six samples contained six monazite grains from which 59 analyses were completed defining an age of 1674 ± 11 Ma (table 3; figure 16e and f). One sample contained a single monazite grain from which seven analyses were completed defining

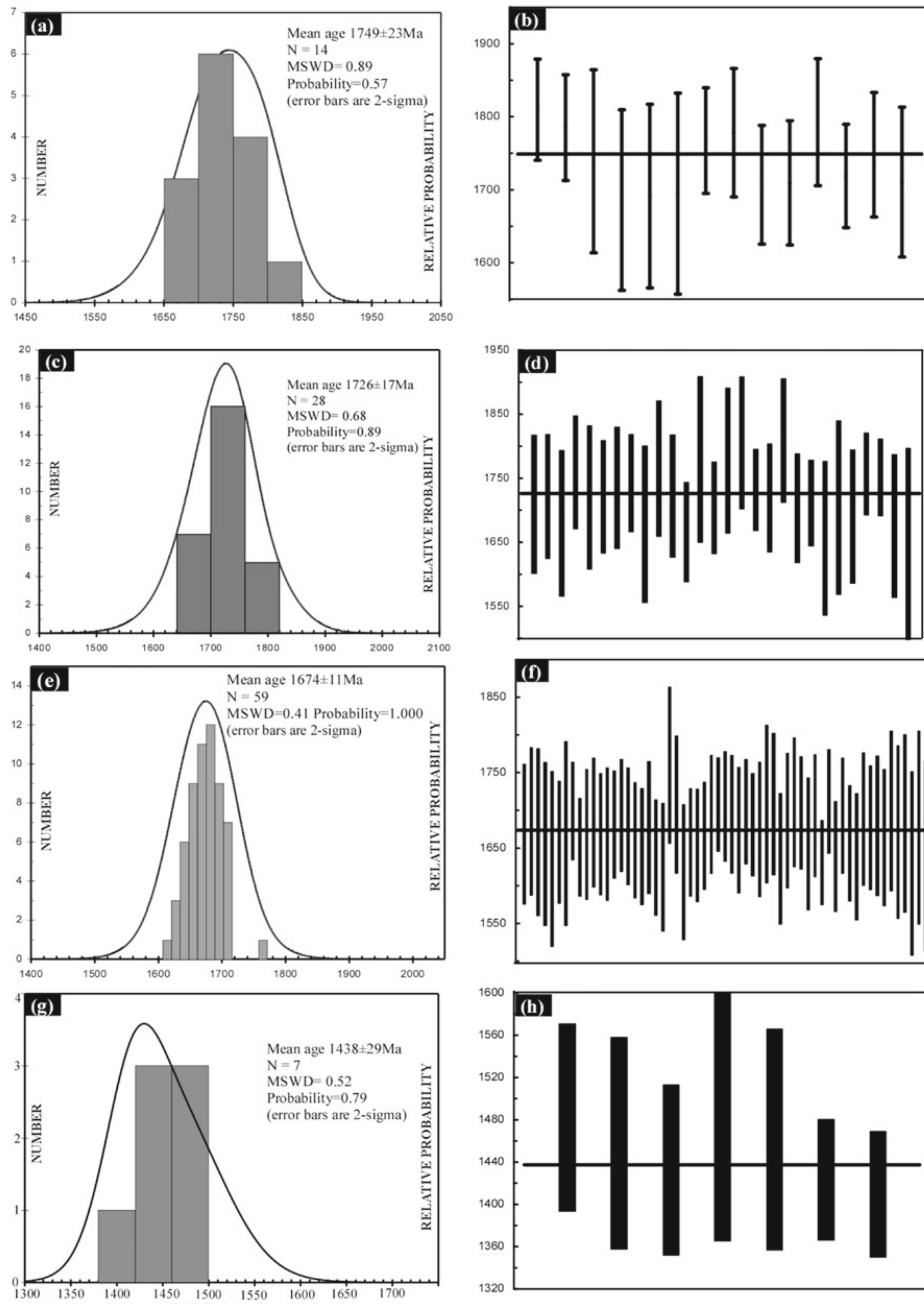

Figure 16. Probability density and weighted average age plots (**a**–**h**) for all samples in which monazite grains were dated within porphyroblasts. These plots were created in Isoplot software (Ludwig 1998). Complete chemical data is shown in tables 4–7.

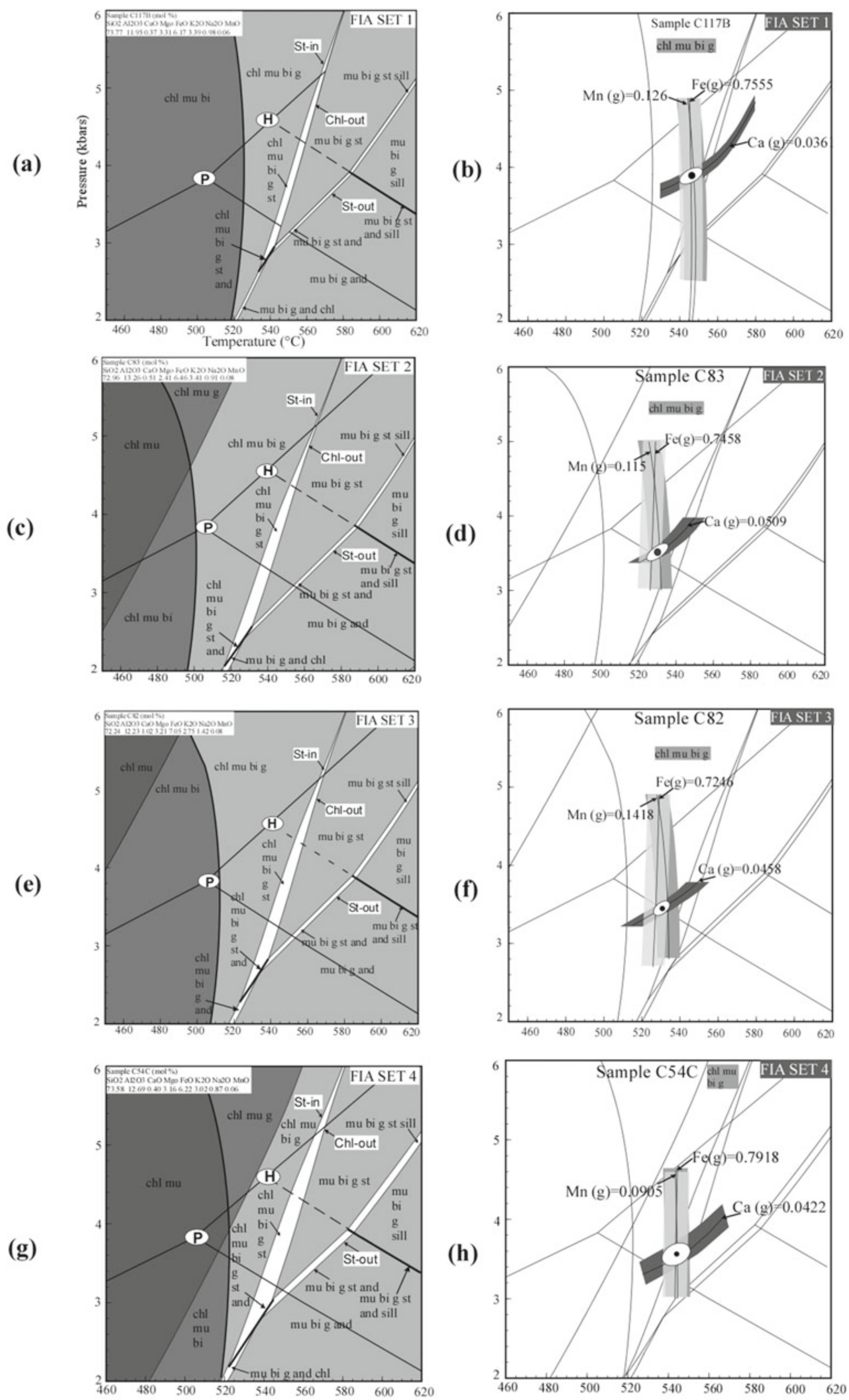

Figure 17. (**a**, **c**, **e** and **f**) P-T pseudosections calculated in the MnNCKFMASH system based on the bulk XRF composition for the samples C117B, C83, C82 and C54C, respectively. It shows the mineral stability fields with dark toned areas representing higher variance value. The bulk composition is displayed on the upper left corner of the diagrams. (**b**, **d**, **f** and **h**) Garnet core isopleths of (X_{Mn}, X_{Ca} and X_{Fe}) in which the compositional contours corresponding to the real composition (microprobe) of garnet core along with their 2-sigma errors indicated as gray-toned think lines (Shah 2010).

an age of 1438 ± 29 Ma (table 3; figure 16g and h). These ages accord to some degree with dates obtained from the porphyroblasts preserving FIA sets 1, 2, 3 and 4 and clearly reflect those events in spite of the fact that there is no real control on the significance.

7.6 *The porphyroblast ages versus matrix ages*

In all the samples that were dated foliations defined by inclusion trails in porphyroblasts are truncated by matrix foliations except in sample C110. Therefore, monazite ages in the matrix have no relevance to the dating of FIAs. In most samples, monazite grains in the matrix foliation gave the same or younger ages than those within the porphyroblasts. Ages range from 1749 ± 23 to 1674 ± 11 Ma (table 3) with one sample preserving a monazite with an approximate FIA 1 age of 1762 Ma and another containing a relic from a foliation within the matrix that predated porphyroblast growth. The younger ages were always a product of reuse or reactivation of old foliations (e.g., Bell *et al.* 2003) or the development of new ones. Consequently, only the ages obtained from monazite grains preserved within porphyroblasts where an FIA control on the significance of that age were used to time deformation and metamorphism (figure 15). However, as mentioned above, it is apparent that most, if not all, of the ages associated with the succession of FIA development are preserved within the matrix. Yet an approach that involves dating monazite grains within the matrix can only ever provide an average age that does not distinguish when deformation commenced or when porphyroblast growth ceased.

7.7 *Role of deformation and its significance for porphyroblast growth*

Nucleation of any mineral phase requires that P–T and bulk composition should be appropriate for that phase to grow. However, deformation is also known to play a vital role in formation of different minerals, particularly porphyroblastic phases (e.g., Bell 1986; Williams 1994; Cihan *et al.* 2006) through its control on sites for the access of nutrients needed for nucleation and growth (Spiess and Bell 1996). The FIA controlled monazite dating described herein reveals ∼90 million years of continuous deformation/metamorphism followed by ∼250 million years of quiescence before orogenesis recommenced for ∼20 million years with little or no change in PT conditions (Shah 2010). What kept this region at similar crustal levels during the 250 million years of quiescence?

The PT conditions and the bulk composition were clearly suitable for the growth of porphyroblasts during the ∼250 Ma between the development of FIAs 3 and 4. Yet no porphyroblastic phases grew during this time and there is no microstructural evidence for any foliations developing. The latter fact is confirmed by dating of monazite grains within the matrix. They reflect the FIA succession and provide no evidence for any deformation between at least 1665 and 1438 Ma. It is now well established that deformation and concurrent metamorphism form cleavage seams by dissolution as well as provide a large range of components essential for the nucleation and growth of porphyroblasts (Bell and Cuff 1989; Spiess and Bell 1996). Deformation provides sites for nucleation and growth, and a means of overcoming the energy barrier for nucleation, in the form of the energy removal from, for example, crenulation hinges (Bell 1986). The lack of porphyroblast growth for this extended ∼250 million year period can be attributed to the lack of crenulation development (Bell *et al.* 2003). When deformation recommenced around ∼1415 Ma, porphyroblasts also began to grow again forming FIA set 4 inclusion trails within garnet, staurolite, andalusite and cordierite porphyroblasts strongly supporting the role of crenulation deformation in porphyroblast growth (e.g., Bell 1986; Cihan *et al.* 2006).

7.8 *Deformation and metamorphism*

The three stages of folding and two stages of metamorphism reported previously from this region were determined from matrix foliation relationship. A much longer history of deformation and metamorphism is preserved by the porphyroblasts. The preservation of four FIA trends with changing directions of shortening from (NE–SW to E–W to SE–NW to NNE–SSW), which range in age from 1760.5 ± 9.7 to 1415 ± 16 Ma has considerable implications for tectonics of this region. The first regional folding episode initiated during FIA set 1 at 1760.5 ± 9.7 Ma and trended NE–SW and approximately coincides with the regional trend of the Cheyenne belt. This is regarded as the suture zone along which the rocks of Colorado and Wyoming province accreted about 1790–1650 Ma ago (Sims *et al.* 2003). Pressure and temperature at this time was about 540°–550°C and 3.8–4.0 kbars, as proposed by the garnet isopleth geothermobarometry. Intersections of Ca, Mg, and Fe isopleths in garnet core, which preserved FIA set 1, indicate that these rocks never got above 4 kbars during the Colorado Orogeny (figure 17a and b).

During the formation of FIA set 2 (centred around 1719.7 ± 6.4 Ma), the pressure and temperature changed slightly to 3.40–3.65 kbar and

525°–537°C (figure 17c and d). F2 regional folds were formed during this stage. Foliation evidence from this period or orogeny is rarely preserved as crenulations in the matrix, due to the effects of rotation and reactivation in the many subsequent deformations. Trondhjemite dikes, which now have a sill like character, were emplaced at ∼1726 ± 15 Ma (Selverstone *et al.* 1997). Intrusion forming W–E trending dikes could occur along the W–E trending vertical foliation that generated this FIA set during gravitational collapse stages of orogenesis when this vertical foliation would have created a plane of weakness that failed (e.g., Bell and Newman 2006). Subsequent reactivation of the compositional layering would have progressively rotated most of them into sub-parallelism with the bedding and disguised any crosscutting relics of the dikes along which they intruded.

FIA set 3 also developed during the Colorado Orogeny (figure 17e and f). The SE–NW trend of this FIA set was created by NE–SW shortening. Previously formed folds were refolded and a new F3, generation were created. The pressure–temperature conditions indicated by garnet isopleth conditions for this period were 3.3–3.6 kbar and 525°–535°C. More staurolite porphyroblasts also grew at this time. In particular, it marks the first appearance of andalusite and cordierite porphyroblasts. Some staurolite porphyroblasts containing FIA set 3 have been partially replaced by andalusite or cordierite suggesting a decrease in pressure accompanied their development. Absolute dating of monazite grains enclosed within the inclusions of these four porphyroblastic phases provide an age of 1674 ± 11 Ma for this period of FIA development which appears to end the Colorado Orogeny. These rocks remained undisturbed for about 250 Ma.

Monazite grains enclosed within the foliations of andalusite and cordierite porphyroblasts containing FIA set 4 give an age of 1420 ± 14 Ma for this period of orogenesis. The tight intersection of Ca, Mn and Fe isopleths in garnet cores indicates that the pressure conditions during this period of orogenesis were similar to those observed at the end of the Colorado Orogeny (figure 17g and h). Large-scale heating event associated with granite emplacement and some deformation at this time is regionally known as the Berthoud Orogeny (Sims *et al.* 2003). FIA set 4 trends NNE–SSW and resulted from NNW–SSE directed shortening. Garnet, staurolite, cordierite and andalusite also grew during this period of orogenesis. Slightly higher temperatures were recorded during this period of orogenesis than previously. Some andalusite and cordierite were formed by replacing staurolite porphyroblasts but most grew as completely new grains. After this period of orogenesis, these rocks were retrogressed, presumably during exhumation. This is revealed by pseudomorphs after staurolite, garnet, cordierite and andalusite (Shah 2010).

7.9 *Regional tectonic implications of Colorado and Berthoud Orogenies*

The metasediments exposed in and around the Big Thompson region of Colorado represent mature sediments deposited in a fore-arc (Condie and Martel 1983) or back-arc setting (Reed *et al.* 1987). Detrital zircon ages suggest a maximum age of 1758 ± 26 Ma for deposition of the Big Thompson sequence (Selverstone *et al.* 2000). Previous researchers (e.g., Selverstone *et al.* 1997; Chamberlain 1998; Shaw *et al.* 2001; Williams *et al.* 1999) suggested protracted metamorphism and deformation associated with the ∼1700 Ma orogeny and local effects due to the ∼1400 Ma orogeny. The evidence presented here for deformation and metamorphism around 1758.8 ± 9 Ma suggests orogenesis commenced around the time of sedimentation. This correlates with the beginning of contractional deformation along the Cheyenne belt, during which time the Colorado province was accreted onto the Archean Wyoming province (Chamberlain 1998). Orogenesis was essentially continuous for about ∼100 Ma and then ceased. FIA data reveal that deformation during 1420 ± 14 Ma Berthoud Orogeny was pervasive, with well-preserved foliations that are continuous with the matrix foliation. However, not a single monazite grain of Berthoud age was found within garnet or staurolite porphyroblasts that could be associated with this event. They were found only in andalusite and cordierite suggesting a slight change in T, P conditions from those forming staurolite was required for further growth of this phase.

Acknowledgements

The authors would like to thank Prof. Tim Bell for his critical comments. Special thanks to Dr Mike Rubenach for help with monazite dating and critical discussions. Funding for this work was provided by the James Cook University.

References

Ali A 2010 The tectono-metamorphic evolution of the Balcooma metamorphic group, north-eastern Australia: A multidisciplinary approach; *J. Metamorph. Geol.* **28** 397–422.

Bell T H 1986 Foliation development and refraction in metamorphic rocks: Reaction of earlier foliations and decrenulation due to shifting patterns of deformation partitioning; *J. Metamorph. Geol.* **4** 421–444.

Bell T H and Cuff C 1989 Dissolution, solution transfer, diffusion *versus* fluid flow and volume loss during deformation/metamorphism; *J. Metamorph. Geol.* **7** 425–448.

Bell T H and Chen A 2002 The development of spiral-shaped inclusion trails during multiple metamorphism and folding; *J. Metamorph. Geol.* **20** 397–412.

Bell T H and Welch P W 2002 Prolonged Acadian Orogenesis: Revelations from FIA controlled monazite dating of foliations in porphyroblasts and matrix American; *J. Sci.* **302** 549–581.

Bell T H and Newman R L 2006 Appalachian Orogenesis: The role of repeated gravitational collapse; In: *Styles of Continental Contraction* (eds) Mazzoli S and Butler R W H; *Geol. Soc. Am. Spec. Paper* **414** 95–118.

Bell T H and Bruce M D 2007 Progressive deformation partitioning and deformation history: Evidence from millipede structures; *J. Struct. Geol.* **29** 18–35.

Bell T H, Forde A and Wang J 1995 A new indicator of movement direction during orogenesis: Measurement technique and application to the Alps; *Terra Nova.* **7** 500–508.

Bell T H, Hickey K A and Upton G J G 1998 Distinguishing and correlating multiple phases of metamorphism across a multiply deformed region using the axes of spiral, staircase and sigmoidally curved inclusion trails in garnet; *J. Metamorph. Geol.* **16** 767–794.

Bell T H, Ham A P and Hickey K A 2003 Early formed regional antiforms and synforms that fold younger matrix schistosities: Their effect on sites of mineral growth; *Tectonophys.* **367** 253–278.

Bell T H, Ham A P and Kim H S 2004 Partitioning of deformation along an orogen and its effects on porphyroblast growth during orogenesis; *J. Struct. Geol.* **26** 825–845.

Bell T H, Ham A P, Hayward N and Hickey KA 2005 On the development of gneiss domes; *Australian J. Earth Sci.* **52** 183–204.

Braddock W A and Cole J C 1979 Precambrian structural relations metamorphic grade, and intrusive rocks along the northeast flank of the Front Range in the Thompson Canyon, Poudre Canyon, and Virginia Dale areas: Field Guide; *Geol. Soc. Am.*, pp. 106–120.

Cavosie A and Selverstone J 2003 Early Proterozoic oceanic crust in the northern Colorado front Range: Implication for crustal growth and initiation of basement faults; *Tectonics* **22** 10–23.

Chamberlain K R 1998 Medicine bow orogeny: Timing of deformation and model of crustal structure produced during continent-arc collision ∼178 Ga, southeastern Wyoming; *Rocky Mountain Geol.* **33** 259–277.

Cherniak D J, Watson E B, Grove M and Harrison T M 2004 Pb diffusion in monazite: A combined RBS/SIMS study; *Geochim. Cosmochim. Acta* **68** 829–840.

Cihan M 2004 The drawbacks of sectioning rocks relative to fabric orientations in the matrix: A case study from the Robertson River Metamorphics (Northern Queensland, Australia); *J. Struct. Geol.* **26** 2157–2174.

Cihan M and Parsons A 2005 The use of porphyroblasts to resolve the history of macro-scale structures: An example from the Robertson River Metamorphics, North- Eastern Australia; *J. Struct. Geol.* **27** 1027–1045.

Cihan M, Evins P, Lisowiec N and Blake K 2006 Time constraints on deformation and metamorphism from EPMA dating of monazite in the Proterozoic Robertson River Metamorphics, NE Australia; *Precambr. Res.* **145** 1–2.

Condie K C and Martel C 1983 Early Proterozoic metasediments from north-central Colorado: Metamorphism, provenance, and tectonic setting; *Geol. Soc. Am. Bull.* **94** 1215–1224.

Dahl P S, Terry M P, Jercinovic M J, Williams M L, Hamilton M A, Foland K A, Clement S M and Friberg L M 2005 Electron probe (Ultrachron) microchronometry of metamorphic monazite: Unraveling the timing of polyphase thermotectonism in the easternmost Wyoming Craton (Black Hills, South Dakota); *Am. Mineral.* **90** 1712–1728.

Gaidies F, Krenn E, de Capitani C and Abart R 2008 Coupling forward modelling of garnet growth with monazite geochronology: An application to the Rappold Complex (Austroalpine crystalline basement); *J. Metamorph. Geol.* **26** 775–793.

Ham A P and Bell T H 2004 Recycling of foliations during folding; *J. Struct. Geol.* **26** 1898–2009.

Hayward N 1990 Determination of early fold axis orientations within multiply deformed rocks using porphyroblasts; *Tectonophys.* **179** 353–369.

Karlstrom K E, Dallmeyer R D and Grambling J A 1997 $^{40}Ar/^{39}Ar$ evidence for 14 Ga regional metamorphism in New Mexico: Implications for thermal evolution of lithosphere in the southwestern US; *J. Geol.* **105** 205–223.

Kelly N M, Clarke G L and Harley S L 2006 Monazite behaviour and age significance in poly-metamorphic high-grade terrains: A case study from the western Musgrave Block, central Australia; *Lithos* **88** 100–134.

Kim H and Bell T H 2005 Combining compositional zoning and foliation intersection axes (FIAs) in garnet to quantitatively determine early P-T-t paths in multiply deformed and metamorphosed schists: North central Massachusetts, USA; *Contrib. Mineral. Petrol.* **149** 141–163.

Ludwig K R 1998 Isoplot/Ex: A geochronological toolkit for Microsoft Excel; *Berkeley Geochronological Center, Spec. Publ.* **1** 43.

Mancktelow N S 1981 Strain variation between quartz grains of different crystallographic orientation in a naturally deformed metasiltstone; *Tectonophys.* **78** 73–84.

Montel J M, Foret S, Veschambre M, Nicolette C and Provost A 1996 Electron microprobe dating of monazite; *Chem. Geol.* **131** 37–53.

Nyman M, Karlstrom K E, Graubard C and Kirby E 1994 Mesozoic contractional orogeny in western North America: Evidence from ca 14 Ga plutons; *Geology* **22** 901–904.

Paquette J L, Nédélec A, Moine B and Rakotondrazafy M 1984 U–Pb, single zircon Pb-evaporation, and Sm–Nd isotopic study of a granulite domain in SE Madagascar; *J. Geol.* **102** 523–538.

Parrish R R 1990 U–Pb dating of monazite and its application to geological problems; *Canadian J. Earth Sci.* **27** 1431–1450.

Pyle J M, Spear F S, Rudnick R I and McDonough W F 2002 Monazite-xenotime-garnet equilibrium in metapelites and a new monazite garnet thermometer; *J. Petrol.* **42** 2083–2107.

Pyle J M, Spear F S, Wark D A, Daniel C G and Storm L C 2005 Contributions to precision and accuracy of chemical ages of monazite; *Am. Mineral.* **90** 547–577.

Reed J C, Bickford M E Jr, Premo W R, Aleinikoff J N and Pallister J 1987 Evolution of the Early Proterozoic Colorado Province: Constraints from U–Pb geochronology; *Geology* **15** 861–865.

Sanislav IV 2010 A long lived metamorphic history in the contact aureole of the Mooselookmeguntic pluton revealed by *in situ* dating of monazite grains preserved as inclusions in staurolite porphyroblasts; *J. Metamorph. Geol.* **29** 251–273.

Sanislav I V and Shah A A 2010 The problem, significance and implications for metamorphism of 60 million years of multiple phases of staurolite growth; *J. Geol. Soc. India* **6** 384–398.

Sanislav IV and Bell T H 2011 The inter-relationships between long-lived metamorphism, pluton emplacement and changes in the direction of bulk shortening during orogenesis; *J. Metamorph. Geol.* **29(5)** 513–536.

Sayab M 2005 Microstructural evidence for N-S shortening in the Mount Isa Inlier (NW Queensland, Australia): The preservation of early W–E-trending foliations in porphyroblasts revealed by independent 3D measurement techniques; *J. Struct. Geol.* **27** 1445–1468.

Sayab M 2006 Decompression through clockwise P-T path: Implications for an early N–S shortening orogenesis in the Mesoproterozoic Mt Isa Inlier (NE Australia); *J. Metamorph. Geol.* **24** 89–105.

Selverstone J, Hodgins M, Shaw C, Aleinikoff J N and Fanning C M 1997 Proterozoic tectonics of the northern Colorado Front Range; In: Geologic history of the Colorado Front Range Denver (eds) Bolyard D W and Sonnenberg S A, *Rocky Mountain Association of Geologist*, pp. 9–18.

Selverstone J, Aleinikoff J, Hodgins M and Fanning C M 2000 Mesoproterozoic reactivation of a Paleoproterozoic transcurrent boundary in the Colorado Front Range: Implications for ca 17 and 14 Ga tectonism; *Rocky Mountain Geol.* **35** 136–162.

Shah A A 2009 FIAs (Foliation Intersection/Inflection Axes) preserved in porphyroblasts, the DNA of deformation: A solution to the puzzle of deformation and metamorphism in the Colorado, Rocky Mountains USA; *Acta Geol. Sin.* **83** 801–840.

Shah A A 2010 Tectono-metamorphic evolution of Big Thompson Canyon Region Colorado Rocky Mountains, USA; Unpublished PhD thesis, James Cook University, B-22.

Shaw C A, Karlstrom K E, Williams M L, Jercinovic M J and McCoy A M 2001 Electron microprobe monazite dating of ca 171–163 Ga and ca 145–138 deformation in the Homestake shear zone, Colorado: Origin and early evolution of a persistent intracontinental tectonic zone; *Geology* **29** 739–742.

Sims Paul K, Stein and Holly J 2003 Tectonic evolution of the Proterozoic Colorado province, Southern Rocky Mountains: A summary and appraisal; *Rocky Mountain Geol.* **38(2)** 183–204.

Spiess R and Bell T H 1996 Microstructural controls on sites of metamorphic reaction: A case study of the inter-relationship between deformation and metamorphism; *European J. Mineral.* **8** 165–186.

Tweto O L 1987 Rock units of the Precambrian basement in Colorado US; *Geological Survey Professional Papers* **1321-A** 54.

Williams M L 1994 Sigmoidal inclusion trails, punctuated fabric development, and interactions between metamorphism and deformation; *J. Metamorph. Geol.* **12** 1–21

Williams M L and Jercinovic M J 2002 Microprobe monazite geochronology: Putting absolute time into microstructural analysis; *J. Struct. Geol.* **24** 1013–1028.

Williams M L, Jercinovic M J and Terry M P 1999 Age mapping and dating of monazite on the electron microprobe: Deconvoluting multistage tectonic histories; *Geology* **27** 1023–1026.

Williams M L, Jercinovic M J, Callum J and Hetherrington 2007 Microprobe monazite geochronology: Understanding geologic processes by integrating composition and chronology; *Ann. Rev. Earth Planet. Sci.* **35** 137–175.

MS received 21 December 2010; revised 6 August 2011; accepted 3 April 2012